J. Fluid Mech. (2014), *vol.* 757, *pp.* 82–113. © Cambridge University Press 2014
doi:10.1017/jfm.2014.485

An inviscid modal interpretation of the 'lift-up' effect

Anubhab Roy[1],‡ **and Ganesh Subramanian**[1],†

[1]Engineering Mechanics Unit, Jawaharlal Nehru Centre for Advanced Scientific Research, Jakkur, Bangalore 560064, India

(Received 8 November 2013; revised 5 August 2014; accepted 20 August 2014; first published online 19 September 2014)

In this paper, we give a modal interpretation of the lift-up effect, one of two well-known mechanisms that lead to an algebraic instability in parallel shearing flows, the other being the Orr mechanism. To this end, we first obtain the two families of continuous spectrum modes that make up the complete spectrum for a non-inflectional velocity profile. One of these families consists of modified versions of the vortex-sheet eigenmodes originally found by Case (*Phys. Fluids*, vol. 3, 1960, pp. 143–148) for plane Couette flow, while the second family consists of singular jet modes first found by Sazonov (*Izv. Acad. Nauk SSSR Atmos. Ocean. Phys.*, vol. 32, 1996, pp. 21–28), again for Couette flow. The two families are used to construct the modal superposition for an arbitrary three-dimensional distribution of vorticity at the initial instant. The so-called non-modal growth that underlies the lift-up effect is associated with an initial condition consisting of rolls, aligned with the streamwise direction, and with a spanwise modulation (that is, a modulation along the vorticity direction of the base-state shearing flow). This growth is shown to arise from an appropriate superposition of the aforementioned continuous spectrum mode families. The modal superposition is then generalized to an inflectional velocity profile by including additional discrete modes associated with the inflection points. Finally, the non-trivial connection between an inviscid eigenmode and the viscous eigenmodes for large but finite Reynolds number, and the relation between the corresponding modal superpositions, is highlighted.

Key words: boundary layer stability, instability, transition to turbulence

1. Introduction

The non-modal behaviour of infinitesimal disturbances in shear flows is attributed mathematically to the non-normal nature of the underlying linearized operator (Schmid & Henningson 2001, p. 101). The two dominant physical mechanisms for non-modal behaviour, leading to short-time algebraic growth, are the Orr mechanism and the lift-up effect. A Reynolds-stress-based argument, which allows for a transfer of energy between the mean flow and an imposed perturbation, is usually offered as

† Email address for correspondence: sganesh@jncasr.ac.in
‡ Present address: School of Chemical and Biomolecular Engineering, Cornell University, Ithaca, NY 14853, USA.

an explanation for the Orr mechanism (see e.g. Farrell 1987; Pradeep & Hussain 2006). The lift-up effect comes in to play only in the presence of a perturbation with an added spanwise variation. (Hereafter, the term 'spanwise variation' is used to refer to the component of variation, of the perturbation field, along the vorticity direction of the base-state shearing flow. The lift-up effect thus requires consideration of a three-dimensional (3D) perturbation, as opposed to the two-dimensional (2D) perturbations that, on account of Squire's theorem, determine the critical Reynolds number for exponential stability (Drazin & Reid 1981).) The commonly offered explanation for the lift-up effect is based on the redistribution of base-state flow momentum in the transverse direction (see Benney & Lin 1960). The mechanism may be best understood for disturbances that are streamwise uniform. For such disturbances, the wall-normal disturbance velocity is time independent, and transports ('lifts up') the mean momentum, riding on its gradient, to produce a streamwise disturbance velocity that grows linearly in time (Schmid & Henningson 2001). In fact, in this limit of no streamwise variation, this mechanism remains unaltered even for finite-amplitude perturbations (Ellingsen & Palm 1975). It is worth noting that, although Ellingsen & Palm (1975) and Landahl (1980) are often credited as being the first to offer an explanation for the 'lift-up' effect based on a solution of the initial value problem, the possibility of algebraic growth of general disturbances in shear flows was noted earlier: by Moffatt (1965) in the context of the linear interaction of a turbulence velocity field with an imposed uniform shear, and by Arnol'd (1972) who attributed the growth to the presence of a Jordan block structure in the linear stability operator. The transient growth associated with the lift-up effect is thought to play an important role in the so-called bypass transition to turbulence for a laminar boundary layer (Andersson, Berggren & Henningson 1999; Reshotko 2001; Tumin & Reshotko 2001). The general mechanism involving the transport of streamwise momentum by transverse velocity fluctuations remains relevant outside the linear stability scenario. For instance, it is responsible for the interplay between streamwise-aligned vortices and streaks that characterize the dynamics in both homogeneous sheared (Rogers & Moin 1987; Lee, Kim & Moin 1990) and near-wall turbulence (Jimenez & Pinelli 1999).

Albeit more cumbersome, a perturbation-vorticity-based stretching and/or tilting mechanism may also be used to explain the lift-up effect and, in fact, lends more insight. This complementary vortex-tilting-based explanation, for a perturbation in the form of a single spanwise Fourier mode, is illustrated in figure 1. In this picture, the lift-up effect arises because the shear in the mean vorticity direction, due to the spanwise variation in the vertical perturbation velocity ($\partial u_z/\partial y$, representative of a 'roll' initial condition), tilts the mean vorticity ($-U'$), producing a linearly growing wall-normal perturbation vorticity (w_z, representative of the vorticity field of a growing streak). Note that a general roll initial condition (as opposed to the single Fourier mode in figure 1) would have an associated $\partial u_y/\partial y$, and would therefore also stretch the base-state vorticity at linear order. There is also a contribution to the streamwise perturbation vorticity, which grows linearly in time, since the w_z generated above is tilted by the mean shear (U') towards the flow direction. But such a contribution is exactly cancelled by a similarly growing contribution that arises from the tilting of the base-state vorticity ($-U'$) due to the spanwise variation of the streamwise perturbation velocity ($\partial u_x/\partial y$ induced by w_z). As a result, only the growing streak survives. Such a cancellation, however, occurs only for plane-parallel flows, in which case the base-state velocity gradient and vorticity are given by U' and $-U'$, respectively. This is no longer the case for curvilinear (vortical) flows, and the

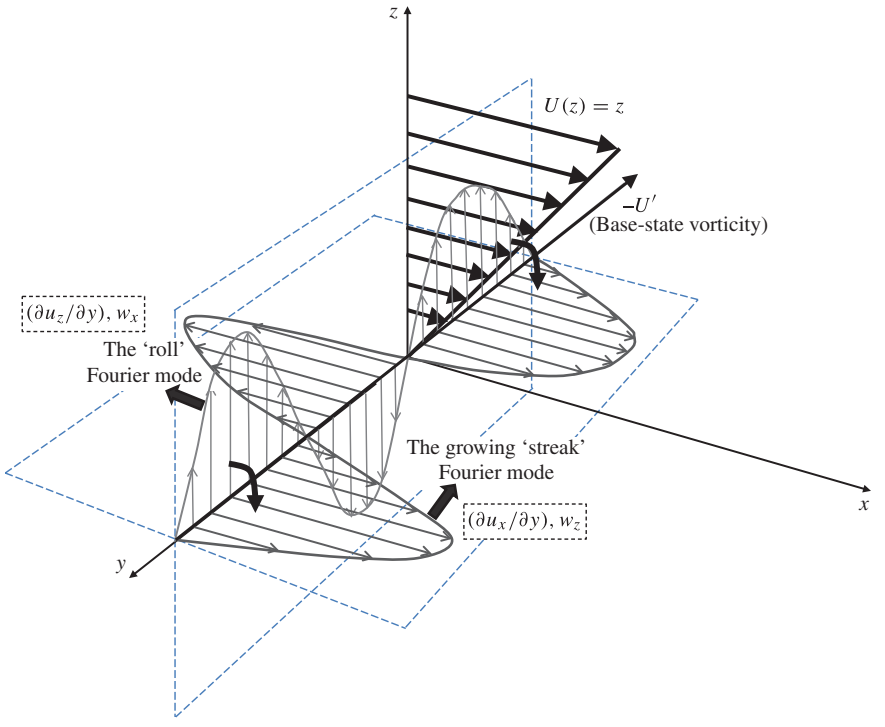

FIGURE 1. (Colour online) Illustration of the algebraic growth in a shear flow associated with the tilting of a spanwise 'roll' Fourier mode (with velocity u_z and vorticity w_x) into a 'streak' Fourier mode (with velocity u_x and vorticity w_z). The bold arrows denote the (linear) shearing flow in the base state $U(z)$, $-U'$ denotes the base-state vorticity, and the curved arrows denote the tilting process. In accordance with the terminology used in the text, a spanwise Fourier mode has its wavevector aligned with the base-state vorticity direction.

second secular contribution noted above persists in these cases (Roy 2013). In fact, the traditional lift-up effect is vanishingly small in regions of negligible base-state vorticity, being identically zero for the limiting case of an irrotational flow induced by a point vortex. In this latter instance, the second secular contribution alone is responsible for algebraic growth, and has been referred as the 'anti-lift-up' effect (Antkowiak & Brancher 2004).

The algebraic growth mechanisms discussed above are essentially of an inviscid origin, with viscosity only leading to an eventual exponential decay of the perturbation kinetic energy on a time scale that, in convective units, is proportional to the Reynolds number (Schmid & Henningson 2001). Thus, there must exist an alternative interpretation of the algebraic growth, in plane-parallel shearing flows, in terms of the dynamics of the inviscid continuous spectra (CS) associated with the Rayleigh operator (Case 1960; Sazonov 1996; Roy & Subramanian 2014). Note that both growth scenarios involve a streamline pattern that changes with time – due to the tilting of wavefronts (constant-vorticity contours) by the base-state shear for the Orr mechanism (see below), and due to the transition of streamwise-aligned rolls to growing streaks for the lift-up effect. The dynamics cannot therefore be described in terms of a single shape-preserving normal mode, and must involve a superposition

of many such modes instead. Such a modal interpretation is most easily seen for the Orr mechanism in Couette flow for 2D perturbations in the plane of shear. Now, the original analyses of the initial value problem, describing the Orr mechanism in Couette flow (see e.g. Farrell 1987), were in terms of Kelvin modes – plane waves with a time-dependent wavevector that is turned by the ambient linear flow (for Couette flow, the wavevector aligns with the gradient direction for long times). However, an equivalent description may be given in terms of a convected superposition of CS modes. In the Kelvin-mode interpretation, the temporal dynamics of the perturbation kinetic energy may be divided into growth and decay phases that are symmetrically located relative to the instant of maximum kinetic energy, and correspond to the wavefronts of the mode having upstream and downstream inclinations, respectively, at the initial time instant. As shown in figure 2(*a*), the shearing flow turns the wavefronts from the former to the latter orientation during the growth phase, and the instant of maximum kinetic energy corresponds to vertical wavefronts aligned with the gradient direction of the base-state shear. Now, the singular modes comprising the CS spectrum for inviscid Couette flow are flow-aligned vortex sheets for 2D perturbations (Case 1960). In the equivalent CS mode interpretation of the Orr mechanism, one considers the action of a shearing flow on an ensemble of such vortex-sheet CS modes staggered in the upstream direction (figure 2*b*). The greater the upstream inclination, the smaller is the degree of coherence (in phase) in the vorticity field, and the smaller is the kinetic energy associated with the initial perturbation. The differential convection due to shear brings the vortex sheets into phase alignment, and the instant of maximum coherence in the gradient direction corresponds to the maximum kinetic energy (Lindzen 1988). Further convection by shear causes the vortex sheets to decohere progressively, leading to a decrease in the kinetic energy for later times. Although not essential, the superposition of vortex sheets may be such as to reproduce the delocalized periodic vorticity field associated with a single Kelvin mode at a given instant, in which case the Kelvin mode and the CS mode interpretations are coincident. The perturbation kinetic energy decays as $O(t^{-2})$ for long times in the inviscid limit. This may be seen by noting that the motion for long times is primarily along the horizontal, and the kinetic energy therefore scales as $O[k_y(t)\psi]^2$, with ψ being the streamfunction and $k_y(t)$ being the (time-dependent) inverse length scale in the gradient direction. Since the vorticity field does not decay in the inviscid case, $\nabla^2\psi = w_z$ may be written in the form $k_y^2(t)\psi \sim O(1)$ with $k_y \sim O(t)$ for long times.

To the best of our knowledge, there exists no modal explanation for the inviscid lift-up effect along the above lines. That is to say, there does not appear to be a representation, in terms of the underlying inviscid CS modes, that accounts for the growth from a streamwise-uniform perturbation, with only a spanwise variation, when there can be no contribution due to the Orr mechanism; and more generally, for any 3D perturbation, when the growth is no longer solely due to the Orr mechanism (Farrell & Ioannou 1993). As mentioned earlier, the usual explanation for the lift-up effect is either based on the linearized inviscid equations of motion, or rather generically attributed to the non-normality of the underlying Orr–Sommerfeld operator, and the resulting non-orthogonality of the discrete viscous modes for large Reynolds number (*Re*) (Reshotko 2001; Schmid & Henningson 2001, p. 101). In the present work we attempt to explain the lift-up effect based on the nature of the inviscid eigenmodes of the underlying Rayleigh operator, and argue that this is superior to the alternative generic explanation in terms of the large-*Re* viscous modes (Reshotko 2001; Schmid & Henningson 2001), particularly because the individual

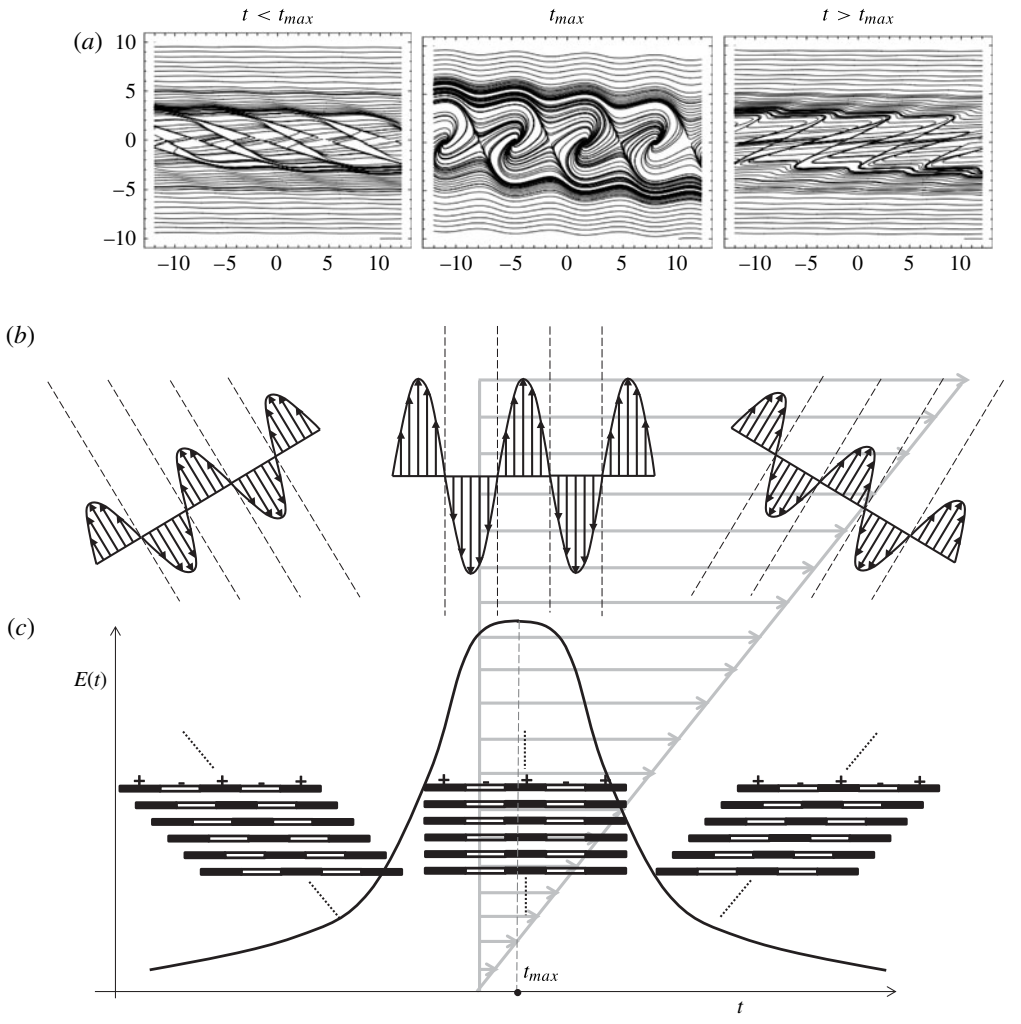

FIGURE 2. Two equivalent interpretations of the Orr mechanism. (*a*) The time-dependent streamline pattern associated with a Kelvin mode, the evolution occurring due to (*b*) tilting of the wavefronts by the background shear. The streamfunction corresponds to the field: $u_x = z + [2(t^2 - t + 1)/(1 + (1 - t)^2)] \cos[x + (1 - t)z]$ and $u_z = [2/(1 + (1 - t)^2)] \cos[x + (1 - t)z]$. (*c*) The evolution of a stack of flow-aligned vortex sheets (singular modes) starting from a configuration staggered in the upstream direction (filled and empty segments denote the harmonic variation of the vortex-sheet strength). The evolution in this interpretation occurs due to the differential convection of the modes by the shear. The superimposed curve shows the time-dependent kinetic energy, with the vertically aligned plane-wave and vortex-sheet configurations corresponding to the maximum kinetic energy at $t = t_{max}$; at this instant, the region where the streamline pattern deviates from that of the base-state shear (*a*) has the greatest vertical extent.

viscous modes do not usually have sensible limits for $Re \to \infty$. The superposition of CS modes that produces a roll initial condition is not as simple as that for the 2D Orr mechanism above, and we therefore arrive at the required superposition after characterizing the general evolution starting from an arbitrary 3D vorticity field at the initial instant.

The paper is organized as follows. In § 2 the problem is formulated for a base state that is an arbitrary plane-parallel shear flow. Herein, the choice of a wavevector-aligned coordinate system, instead of the usual flow-aligned one, allows one to simplify the normal-mode analysis. Next, in § 3, based on the existing knowledge of the 3D CS modes for Couette flow (Sazonov 1996) and the 2D CS modes for nonlinear shear flows (Balmforth & Morrison 1995), the two families of CS eigenfunctions, for a nonlinear shear flow, are obtained. This description is next used in § 4 to develop an inviscid modal superposition. In § 4.1, such a superposition is developed for an arbitrary initial condition. Next, in § 4.2, the superposition for a specific 'roll' initial condition is used to exhibit the algebraic instability corresponding to the 'lift-up' effect. Since exponentially unstable modes are not responsible for the 'lift-up' effect, the analysis above is developed for a non-inflectional smooth velocity profile in which case the spectrum is absolutely continuous (see Lin 1955; Fadeev 1971). In § 4.3, the modal superposition is generalized to accommodate inflectional velocity profiles by allowing for additional pairs of discrete modes associated with each inflection point. The inviscid modal interpretation of the 'lift-up' effect given here, in a sense, complements an existing qualitative interpretation in terms of non-orthogonal viscous discrete modes (Schmid & Henningson 2001, pp. 106–107), although the relation between the two is non-trivial. Thus, § 5 is devoted to a discussion of the connection between an inviscid eigenmode and the discrete viscous modes, for large but finite Re, in the context of the analytically solvable problem of Couette flow. Section 6 concludes by summarizing the main findings of this paper.

2. Problem formulation

Consider a normal mode imposed on a unidirectional shearing flow with velocity profile $U(z)$. It will be seen in § 4 that the modal superposition takes its simplest form in wavevector-aligned coordinates, and we will therefore obtain the expressions for the singular normal modes in a wavevector-aligned coordinate system (x', y', z) instead of the usual flow-aligned coordinate system (x, y, z) with x, y and z in the latter case corresponding, respectively, to the flow, vorticity and gradient directions of the base state. The two coordinate systems are related by a rotation about the z-axis as shown in figure 3. Since the flow and vorticity directions are homogeneous, the wavevector lies in the flow–vorticity plane with $\boldsymbol{k} \equiv (k_x, k_y)$, and if ψ is the angle made by $\boldsymbol{k}$ with the flow direction, we have the following relations between the coordinate systems:

$$(k_x = k\cos\psi,\, k_y = -k\sin\psi), \quad \left(k_{x'} = k = \sqrt{k_x^2 + k_y^2},\, k_{y'} = 0\right), \tag{2.1a,b}$$

$$u_{x'} = u_x\cos\psi - u_y\sin\psi, \quad u_{y'} = u_y\cos\psi + u_x\sin\psi, \quad u_z' = u_z. \tag{2.2a–c}$$

A normal mode will have the general form $\hat{F}(z)\,\mathrm{e}^{\mathrm{i}[k_x(x-ct)+k_y y]}$ in flow-aligned coordinates, and the form $\hat{F}(z)\,\mathrm{e}^{\mathrm{i}k(x'-c't)}$ in wavevector-aligned coordinates, with c and c' being the phase speeds in the x and x' directions, respectively, and $\hat{F}(z)$ denoting the z-dependent amplitude of the relevant perturbation field. The linearized equations of motion for the normal-mode amplitudes may be derived in the usual manner (Drazin & Reid 1981). These, together with the continuity equation and the expressions for the different components of the perturbation vorticity field, in the two coordinate systems, are summarized in table 1; here, D denotes $\mathrm{d}/\mathrm{d}z$.

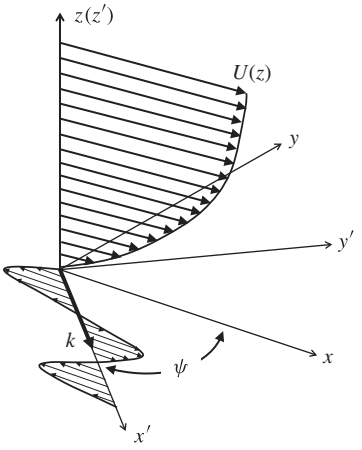

FIGURE 3. Shear flow in the flow-aligned and wavevector-aligned coordinate systems.

Flow-aligned	Wavevector-aligned
Momentum equation	
$\mathrm{i}k_x(U-c)\hat{u}_x + \hat{u}_z U' = -\mathrm{i}k_x\hat{p}$	$\mathrm{i}k_x(U-c)\hat{u}_{x'} + \hat{u}_z U'\cos\psi = -\mathrm{i}k\hat{p}$
$\mathrm{i}k_x(U-c)\hat{u}_y = -\mathrm{i}k_y\hat{p}$	$\mathrm{i}k_x(U-c)\hat{u}_{y'} + \hat{u}_z U'\sin\psi = 0$
$\mathrm{i}k_x(U-c)\hat{u}_z = -\mathrm{D}\hat{p}$	$\mathrm{i}k_x(U-c)\hat{u}_z = -\mathrm{D}\hat{p}$
$\mathrm{i}k_x\hat{u}_x + \mathrm{i}k_y\hat{u}_y + \mathrm{D}\hat{u}_z = 0$	$\mathrm{i}k\hat{u}_{x'} + \mathrm{D}\hat{u}_z = 0$
Vorticity components	
$\hat{w}_z = \mathrm{i}k_x\hat{u}_y - \mathrm{i}k_y\hat{u}_x$	$\hat{w}_z = \mathrm{i}k\hat{u}_{y'}$
$\hat{w}_x = \mathrm{i}k_y\hat{u}_z - \mathrm{D}\hat{u}_y$	$\hat{w}_{x'} = -\mathrm{D}\hat{u}_{y'}$
$\hat{w}_y = \mathrm{D}\hat{u}_x - \mathrm{i}k_x\hat{u}_z$	$\hat{w}_{y'} = \mathrm{D}\hat{u}_{x'} - \mathrm{i}k\hat{u}_z$
$(\mathrm{D}^2 - k^2)\hat{u}_z = \mathrm{i}k_y\hat{w}_x - \mathrm{i}k_x\hat{w}_y$	$(\mathrm{D}^2 - k^2)\hat{u}_z = -\mathrm{i}k\hat{w}_{y'}$

TABLE 1. Relevant equations in the flow-aligned and wavevector-aligned coordinate systems.

From the governing equations above, one may derive the following equations governing the normal velocity and vorticity fields:

$$(U-c)(\mathrm{D}^2 - k^2)\hat{u}_z - U''\hat{u}_z = 0, \tag{2.3}$$

$$k_x(U-c)\hat{w}_z = U' k_y \hat{u}_z. \tag{2.4}$$

Equations (2.3) and (2.4) are the Rayleigh and the (inviscid) Squire equations for 3D perturbations (Drazin & Reid 1981, p. 129). Note that (2.3) is identical to that for 2D perturbations except for k_x being replaced by the total wavenumber k. The addition of $O(1/Re)$ viscous terms in (2.3) and (2.4) leads to the Orr–Sommerfeld–Squire system, whose properties have been discussed in detail (see e.g. Schmid & Henningson 2001, pp. 56–61).

In § 3, it is shown that the system (2.3)–(2.4) supports two families of continuous spectrum (CS) modes. For non-inflectional velocity profiles that possess only a CS (Fadeev 1971), it will be shown, by construction, that these two CS mode families

constitute a complete set of (singular) eigenfunctions capable of representing an arbitrary initial vorticity distribution. One of the families arises from the homogeneous solution of (2.3), with the resulting normal velocity field forcing the Squire equation; these are the Rayleigh or, as we shall term them, the Λ_1 modes. The second family is a homogeneous solution of (2.4), with a velocity field restricted to the flow–vorticity plane. These inviscid Squire modes will be termed the Λ_2 modes in what follows. The terminology is motivated by our identification of these families with the CS mode families found recently in the case of a Rankine vortex (Roy & Subramanian 2014). Although there are differences in detail in the structure of the vorticity fields in the two cases, there is an exact analogy in the 2D limit (for the parallel flow case, this corresponds to $\psi = 0$, and for the vortex case, the limit implies the absence of any modulation along the axis of rotation).

3. The continuous spectrum of the linearized Euler equations

3.1. *The Λ_1 family – inclined Case vortex sheets*

We first write (2.3) in terms of the vorticity component, $\hat{w}_{y'}$, in the form

$$\mathrm{i}k(U-c)\hat{w}_{y'} = -U''\hat{u}_z. \tag{3.1}$$

Assuming c to be in the base-state range of velocities, one may write $c = U(z_c)$, with z_c denoting the critical level where the fluid in the base state moves at the same speed as the perturbation, and (3.1) takes the form

$$[U(z) - U(z_c)]\hat{w}_{y'} = \frac{\mathrm{i}}{k}U''\hat{u}_z. \tag{3.2}$$

Now, $[U(z) - U(z_c)] \approx U'(z_c)(z - z_c)$ for z close to z_c, and (3.2) therefore has the homogeneous solution $\hat{w}_{y'} \propto \delta(z - z_c)$, where we have used the generalized function identity $(z - z_c)\delta(z - z_c) = 0$ (Lighthill 1958); in the hydrodynamical context, this was first recognized by Case (1960) for the case of Couette flow ($U(z) \propto z$). The general solution of (3.1) may now be written as the sum of the above homogeneous solution and a particular solution driven by U'', and this leads to the total $\hat{w}_{y'}$ field associated with a Λ_1 CS mode. From (2.4), using $\hat{w}_z = \mathrm{i}k\hat{u}_{y'}$, the normal velocity field induced by the $\hat{w}_{y'}$ field is seen to lead to a non-zero $\hat{u}_{y'}$. A 3D Λ_1 CS mode is therefore characterized by

$$\hat{w}^{\Lambda_1}_{y',k} = -\mathcal{C}_1\delta(z - z_c) + \mathcal{P}\frac{\mathrm{i}}{k}\frac{U''(z)\hat{u}_{z,k}}{U(z) - c}, \tag{3.3}$$

$$\hat{u}^{\Lambda_1}_{y',k} = \mathcal{P}\frac{k_y}{\mathrm{i}kk_x}\frac{U'(z)\hat{u}_{z,k}}{U(z) - c}, \tag{3.4}$$

where the subscript k denotes quantities associated with a single Fourier mode of wavenumber k and $\mathcal{P}$ implies a Cauchy principal value (PV) interpretation. Both the $\hat{w}_{y'}$ and $\hat{u}_{y'}$ fields are singular at $z = z_c$. Here, $z_c = U^{-1}(c)$, and the requirement that z_c lie within the domain implies that c spans the base-state range of velocities – the interval corresponding to the CS associated with the Rayleigh equation.

In (3.3) the homogeneous solution denotes a localized vortex-sheet contribution. A flow-aligned vortex sheet, on account of its infinitesimal thickness, satisfies the essential requirement of a normal mode, that of remaining undistorted by the

base-state shear. For a nonlinear shear flow ($U'' \neq 0$), the particular solution in (3.3) denotes an additional non-local contribution that arises due to the induction mechanism associated with convection of the inhomogeneous base-state vorticity gradient by the perturbation normal velocity ($\hat{u}_{z,k}$) induced, in part, by the vortex sheet. In a reference frame translating with c, the convection of $\hat{w}_{y'}$ by the base-state shear becomes small, being $O(z - z_c)$ for z close to z_c, while the rate of induction remains finite for a non-zero $U''(z_c)$ provided $\hat{u}_{z,k}$ also remains finite. Thus, the non-local contribution to $\hat{w}_{y'}$ needs to increase as $(z - z_c)^{-1}$ in order for a steady balance (in the chosen reference frame) between the two mechanisms to prevail close to z_c. The PV interpretation of this singularity in (3.3) may be regarded as a self-consistency requirement, since it corresponds to a finite $\hat{u}_{z,k}$ induced at the critical level due to the cancelling singularities in the $\hat{w}_{y'}$ field for $z \to z_c^{\pm}$. The expression (3.3) is identical to the structure of the 2D CS modes (with $k_y = 0$) originally identified by Case (1959) in the context of perturbations to the electron velocity distribution, as governed by the Vlasov equation, and discussed in more detail in the specific context of inviscid hydrodynamic stability by Balmforth & Morrison (1995). In the hydrodynamical context, (3.3) and (3.4) may be regarded as the generalization of the vortex sheets, originally found by Case (1960) for 2D perturbations, to the case of an inclined wavevector.

For a 2D CS mode, $\hat{u}_{y',k} = 0$, and the vortex-sheet contribution in (3.3) induces a discontinuity in slope of $\hat{u}_z$ across the critical level. As evident from (3.4), the 3D Λ_1 mode has an additional stronger singularity in the $\hat{u}_{y'}$ field. This component is PV-singular at $z = z_c$, and arises from (2.4) due to the tilting of the base-state vorticity field, which occurs at a finite rate even at the critical level. The PV-singular terms in a single Λ_1 CS mode imply that the evolution towards such a mode, starting from a vortex-sheet initial condition (due to, say, a localized baroclinic forcing at the initial instant; see Kelbert & Sazonov 1996), has a non-trivial character. For the 2D case, it has been shown that, although the velocity in most of the domain converges to that of a propagating CS mode for long times, there remains an unsteady region surrounding the critical level, with an extent of $O(1/t)$ (t being the time) where the tangential velocity increases as $\ln t$, and thereby departs from that associated with the steady singular mode (Dickinson 1970; Tung 1983). For Couette flow, the PV-singular term in the vorticity field vanishes, and the $\hat{w}_{y',k}$ eigenmode is exactly a vortex sheet. The perturbation vorticity field, however, continues to be 3D on account of $\hat{u}_{y',k}$. The PV-singular $u_{y',k}$ field arises from vortex tilting and not from a base-state vorticity gradient, and therefore, persists even for Couette flow (see Sazonov 1996).

Inverting the relation, $(\mathrm{D}^2 - k^2)\hat{u}_{z,k} = (-\mathrm{i}k\hat{w}_{y',k})$ from table 1, in terms of a Green's function, we have the following expression for the normal component of the perturbation velocity field associated with $\hat{w}^{\Lambda_1}_{y',k}$ in (3.3):

$$\hat{u}^{\Lambda_1}_{z,k}(z; z_c) = -\mathrm{i}k\mathcal{C}_1\mathcal{G}(z; z_c) + \frac{\mathrm{i}}{k}\,\mathcal{P}\int_{-1}^{1} \frac{\mathcal{G}(z; z')U''(z')\hat{u}^{\Lambda_1}_{z,k}(z; z')}{U(z') - U(z_c)}\,\mathrm{d}z', \tag{3.5}$$

where $\mathcal{G}(z; z_c)$ is the Green's function. For a bounded domain, $z \in [-1, 1]$, with the boundary conditions $\hat{u}^{\Lambda_1}_{z,k}(\pm 1; z_c) = 0$, the Green's function is given by

$$\mathcal{G}(z; z_c) = -\frac{\sinh(k(1 - z_>))\,\sinh(k(1 + z_<))}{k\sinh 2k}, \tag{3.6}$$

with $z_<$ ($z_>$) denoting the smaller (larger) of z and z_c. On normalizing the total y' vorticity associated with a given Λ_1 mode,

$$\int_{-1}^{1} \hat{w}^{\Lambda_1}_{y',k}(z'; z_c)\,\mathrm{d}z' = \Sigma_1, \tag{3.7}$$

one may characterize each Λ_1 CS mode by the following expressions for the vorticity and velocity fields:

$$\hat{w}^{\Lambda_1}_{y',k}(z; z_c) = \left\{\Sigma_1 - \frac{\mathrm{i}}{k}\mathcal{P}\int_{-1}^{1}\frac{U''(z')\hat{u}^{\Lambda_1}_{z,k}(z'; z_c)}{U(z') - U(z_c)}\,\mathrm{d}z'\right\}\delta(z - z_c) + \mathcal{P}\frac{\mathrm{i}}{k}\frac{U''(z)\hat{u}^{\Lambda_1}_{z,k}(z; z_c)}{U(z) - U(z_c)}, \tag{3.8}$$

$$\hat{u}^{\Lambda_1}_{z,k}(z; z_c) = -\mathrm{i}kC_1\mathcal{G}(z; z_c) + \frac{\mathrm{i}}{k}\int_{-1}^{1} U''(z')\hat{u}^{\Lambda_1}_{z,k}(z'; z_c)\frac{\mathcal{G}(z; z') - \mathcal{G}(z; z_c)}{U(z') - U(z_c)}\,\mathrm{d}z', \tag{3.9}$$

$$\hat{u}^{\Lambda_1}_{y',k}(z; z_c) = \mathcal{P}\frac{k_y U'(z)\hat{u}^{\Lambda_1}_{z,k}(z; z_c)}{\mathrm{i}kk_x(U(z) - c)}. \tag{3.10}$$

Note that the normalization based on Σ_1 above assumes the total y' vorticity associated with the eigenmode to be non-zero (see Balmforth & Morrison 1995). This may not always be the case (see e.g. Sazonov 1989; Roy & Subramanian 2014), but in the analysis here we will neglect these instances, regarding them as exceptional.

It is important to note that, in the inviscid framework, the general character of the Λ_1 modes remains the same regardless of whether the domain is bounded or unbounded. This is due to the localization of the perturbation vorticity field at the critical level. The vortex-sheet contribution in (3.3) evidently remains the same for both bounded and unbounded domains. The change in the induced velocity field implies that the non-local PV-singular contribution to the vorticity field in (3.3), and that corresponding to (3.4), will be different in the two cases. However, the induced velocity fields for a bounded and unbounded domain only differ by an irrotational component needed to satisfy the impenetrability conditions at the boundaries in the former case. Since this irrotational contribution is regular within the domain, the structure of the PV-singular term in the vorticity field at $z = z_c$ remains unaltered. There is therefore no real loss of generality in writing down (3.8)–(3.10) using the Green's function defined by (3.6). The only change in going to an unbounded domain would be to use the relevant Green's function, given by $\mathcal{G}(z; z_c) = -\exp(-k|z - z_c|)/2$ and satisfying the decay conditions for $z \to \pm\infty$, and to extend the range of integration in (3.8)–(3.10) to $(-\infty, \infty)$.

3.2. *The Λ_2 family – Squire jets*

The Λ_2 CS modes are homogeneous solutions of (2.4) with $\hat{u}_{y'}$ being the only non-zero velocity component in wavevector-aligned coordinates. Since the Squire operator in (2.4) is just the multiplication operator, use of the identity $(z - z_c)\delta(z - z_c) = 0$ implies that $\hat{u}^{\Lambda_2}_{y',k} = \delta(z - z_c)$. One may accordingly term such modes as 'Squire jets'. Note that since $\hat{w}_{y',k} = \hat{u}_{z,k} = 0$, the Rayleigh equation (3.2) is trivially satisfied in these cases. Thus, we have a Λ_2 CS mode being characterized by the following velocity and vorticity fields:

$$\hat{u}^{\Lambda_2}_{y',k}(z; z_c) \;=\; \Sigma_2\delta(z - z_c), \tag{3.11}$$

$$\hat{w}^{\Lambda_2}_{z,k}(z;z_c) = \mathrm{i}k\Sigma_2\delta(z-z_c), \tag{3.12}$$

$$\hat{w}^{\Lambda_2}_{x',k}(z;z_c) = -\Sigma_2\delta'(z-z_c). \tag{3.13}$$

Here, again, z_c is such that c spans the base-state range of velocities – the inviscid Squire CS. The normalization $\Sigma_2 = \int_{-1}^{1} u^{\Lambda_2}_{y',k}(z';z_c)\,\mathrm{d}z'$ used above may be interpreted as the volume flux per (half-)wavelength associated with each mode. These modes were originally written down by Sazonov (1996) while studying the evolution of 3D disturbances in Couette flow. The localized perturbation velocity field implies, however, that the evolution of such a mode only depends on the velocity gradient at the critical level, and therefore, (3.11)–(3.13) remain solutions of the linearized equations of motion for an arbitrary nonlinear base-state velocity profile. In addition, the localization of the velocity field at $z = z_c$ implies the Λ_2 modes remain the same for both bounded and unbounded domains.

To summarize, the velocity and vorticity fields associated with the Λ_1 and Λ_2 CS modes are given by (3.8)–(3.10) and (3.11)–(3.13), respectively, with z_c spanning the domain. As shown originally by Case (1960) for Couette flow, and later by Balmforth & Morrison (1995) for a general nonlinear shearing flow, an arbitrary vortical perturbation in two dimensions (that is, with $k_y = 0$, and the perturbation velocity field restricted to the xz plane) may be expressed as a superposition of the Λ_1 CS modes alone. Thus, these are the only modes needed for an interpretation of the Orr mechanism in two dimensions, and the schematic in figure 2 is an example of such an interpretation for Couette flow. On the other hand, the Λ_2 modes come into play only for a perturbation that includes a spanwise variation, and, as will be seen in § 4.2, are crucial to explaining the lift-up effect.

Finally, it must be noted that, unlike the inviscid eigenfunctions above, there are crucial differences in the nature of the viscous spectrum and the associated eigenfunctions between bounded and unbounded domains. For a bounded domain, as originally argued by Lin (1955), the spectrum of the Orr–Sommerfeld equation is purely discrete. The spectrum for the unbounded case, however, depends on the nature of the base-state velocity profile. On the one hand, considering a semi-infinite domain with a velocity profile that approaches a uniform flow at infinity leads to the appearance of a viscous CS consisting of eigenfunctions that oscillate finitely rather than decay at infinity. This was originally found numerically for the Blasius profile (Mack 1976), and appears to be a generic feature of Blasius-like profiles in a semi-infinite domain (Murdock & Stewartson 1977); the interval corresponding to the CS for such profiles has also been established (Grosch & Salwen 1978, 1981). On the other hand, for velocity profiles that asymptote to a finite shear at infinity, for instance, unbounded Couette flow ($U(z) \propto z$, $z \epsilon (-\infty, \infty)$), the spectrum remains discrete except for disturbances that only have a spanwise variation. At least for unbounded Couette flow, there is neither a discrete nor a continuous spectrum in the absence of boundaries, and as shown in § 5, the crucial role of boundaries in this case leads to a non-trivial relation between the inviscid CS modes, analysed above in §§ 3.1 and 3.2, and the viscous modes for large but finite Re. In particular, each CS mode may be sensibly interpreted only as the limiting form of a viscous wavepacket, since the individual viscous eigenmodes do not approach sensible limiting forms for $Re \to \infty$.

4. The modal representation of a vortical initial condition

4.1. *A general initial condition*

The determination of the arbitrary time evolution of a general initial velocity field $\boldsymbol{u}(\boldsymbol{x}, 0)$ may be reduced to the problem of the evolution of a single Fourier mode in

the wavevector-aligned coordinate system as follows:

$$\begin{aligned}\boldsymbol{u}(\boldsymbol{x},\,t) \;&=\; \int_{-\infty}^{\infty}\int_{-\infty}^{\infty} \mathrm{d}k_x\,\mathrm{d}k_y\,\hat{\boldsymbol{u}}_k(z,\,t)\,\mathrm{e}^{\mathrm{i}(k_x x+k_y y)},\\ &=\; \int_{-\infty}^{\infty}\int_{-\infty}^{\infty} \mathrm{d}k_x\,\mathrm{d}k_y\{\hat{u}_{x,k}(z,\,t)\hat{\boldsymbol{x}}+\hat{u}_{y,k}(z,\,t)\hat{\boldsymbol{y}}+\hat{u}_{z,k}(z,\,t)\hat{\boldsymbol{z}}\}\,\mathrm{e}^{\mathrm{i}(k_x x+k_y y)}, \qquad (4.1)\end{aligned}$$

in terms of the Fourier modes in flow-aligned coordinates. Here $[\hat{\boldsymbol{x}},\hat{\boldsymbol{y}},\hat{\boldsymbol{z}}]$ denotes the unit vector triad aligned with the base-state flow, gradient and vorticity directions. Transforming to wavevector-aligned coordinates, and with the aid of the continuity equation, one obtains

$$\begin{aligned}\boldsymbol{u}(\boldsymbol{x},\,t) \;=\; \int_{-\infty}^{\infty}\int_{-\infty}^{\infty} \mathrm{d}k_x\,\mathrm{d}k_y\,&\left[\left\{\frac{\mathrm{i}}{k}\mathrm{D}\hat{u}_{z,k}(z,\,t)\cos\psi+\hat{u}_{y',k}(z,\,t)\sin\psi\right\}\hat{\boldsymbol{x}}\right.\\ &\left.+\left\{\hat{u}_{y',k}(z,\,t)\cos\psi-\frac{\mathrm{i}}{k}\mathrm{D}\hat{u}_{z,k}(z,\,t)\sin\psi\right\}\hat{\boldsymbol{y}}+\hat{u}_{z,k}(z,\,t)\hat{\boldsymbol{z}}\right]\mathrm{e}^{\mathrm{i}(k_x x+k_y y)}, \qquad (4.2)\end{aligned}$$

where we have used that $\hat{u}_{z',k}(z,\,t)=\hat{u}_{z,k}(z,\,t)$.

It is clear from (4.2) that a description of $\hat{u}_{z,k}(z,\,t)$ (or, equivalently, $\hat{w}_{y',k}(z,\,t)$) and $\hat{u}_{y',k}(z,\,t)$ for a given $\boldsymbol{k}$, in terms of a superposition over the singular eigenfunctions of the aforementioned Λ_1 and Λ_2 families, would lead to the required modal representation for an arbitrary $\boldsymbol{u}(\boldsymbol{x},\,t)$ via the Fourier integral representation. Hence, we now examine the evolution of a single Fourier mode that, at the initial instant, has a vertical structure given by $(\hat{w}_{y',k}(z,\,0),\,\hat{u}_{y',k}(z,\,0))\equiv(\mathscr{Q}_1(z),\,\mathscr{Q}_2(z))$. This choice of perturbation fields is motivated by the structure of the Λ_2 family. As shown below, the fact that the Λ_2 eigenmodes have $\hat{w}_{y',k}=0$ allows one to arrive at the modal superposition in a simple sequential manner. The continuity equation, and the kinematic relation between streamfunction and vorticity, may be used to obtain the remaining disturbance velocity fields in terms $\hat{w}'_y$ and $\hat{u}'_y$. The choice of perturbation fields above is in contrast to the usual choice of the wall-normal velocity ($\hat{u}_{z,k}$) and the wall-normal vorticity ($\hat{w}_{z,k}$) fields (see e.g. Schmid & Henningson 2001). However, the two choices may be readily related: $\hat{u}_{z,k}(z,\,0)$ is related to $\hat{w}_{y',k}(z,\,0)$ via the Poisson equation, so $(\mathrm{D}^2-k^2)\hat{u}_{z,k}(z,\,0)=-\mathrm{i}k\mathscr{Q}_1(z)$; and $\hat{w}_{z,k}(z,\,0)=\mathrm{i}kQ_2(z)$ (see table 1).

To construct the ensemble of the Λ_i modes ($i=1,\,2$) that reproduce the above initial condition, for a fixed $\boldsymbol{k}$, we now exploit the fact that the Λ_2 family is devoid of $w_{y'}$. As a result, one may construct the required modal superposition by first determining the superposition of Λ_1 modes required to represent $\hat{w}_{y',k}(z,\,0)\equiv\mathscr{Q}_1(z)$. That is, we have

$$\mathscr{Q}_1(z)=\int_{-1}^{1} A^{\Lambda_1}(z')\hat{w}^{\Lambda_1}_{y',k}(z;\,z')\,\mathrm{d}z', \qquad (4.3)$$

where $A^{\Lambda_1}(z')$ is the unknown amplitude distribution that needs to be determined. Provided one knows A^{Λ_1}, the vorticity field $\hat{w}_{y',k}$, at an arbitrary time instant, follows immediately on convecting each of the Λ_1 modes with the base-state velocity at its critical level. Thus,

$$\hat{w}_{y',k}(z,\,t)=\int_{-1}^{1} A^{\Lambda_1}(z')\hat{w}^{\Lambda_1}_{y',k}(z;\,z')\,\mathrm{e}^{-\mathrm{i}k_x U(z')t}\,\mathrm{d}z', \qquad (4.4)$$

with an analogous equation for $\hat{u}_{z,k}(z,\,t)$. Using (3.8) with $z_c = z'$ for $\hat{w}^{\Lambda_1}_{y',k}(z;\,z')$ in (4.3), one obtains the following Cauchy integral equation (Gakhov 1990) to be solved for $A^{\Lambda_1}(z)$:

$$\mathscr{Q}_1(z) = A^{\Lambda_1}(z)\left\{\Sigma_1 - \frac{\mathrm{i}}{k}\,\mathcal{P}\int_{-1}^{1}\frac{U''(z')\hat{u}^{\Lambda_1}_{z,k}(z';\,z)}{U(z')-U(z)}\,\mathrm{d}z'\right\} - \frac{\mathrm{i}}{k}U''(z)\,\mathcal{P}\int_{-1}^{1}\frac{A^{\Lambda_1}(z')\hat{u}^{\Lambda_1}_{z,k}(z;\,z')}{U(z')-U(z)}\,\mathrm{d}z', \tag{4.5}$$

where the symbol $\mathcal{P}$ implies that the integrals must be interpreted in the sense of a Cauchy PV. The solution of an analogous integral equation in plasma physics, which arose from a governing Vlasov equation, was originally accomplished by Case (1959) in terms of the solution of a Riemann–Hilbert problem in the complex plane (Gakhov 1990). The solutions of similar integral equations arising in the context of both parallel shearing flows (Balmforth & Morrison 1995) and vortical flows (Roy & Subramanian 2014) have also been obtained. We refer the reader to these references for details of the solution procedure, and write down the final expression for $A^{\Lambda_1}(z)$:

$$A^{\Lambda_1}(z) = \frac{1}{\epsilon_R^2+\epsilon_L^2}\left[\epsilon_R\mathscr{Q}_1(z) - \frac{\epsilon_L U'}{\hat{u}^{\Lambda_1}_z(z;\,z)}\,\mathcal{P}\int_{-1}^{1}\frac{\hat{u}^{\Lambda_1}_z(z;\,z')\mathscr{Q}_1(z')}{U(z')-U(z)}\,\mathrm{d}z'\right], \tag{4.6}$$

where

$$\epsilon_R = \Sigma_1 - \frac{\mathrm{i}}{k}\,\mathcal{P}\int_{-1}^{1}\frac{U''(z')\hat{u}^{\Lambda_1}_z(z;\,z')}{U(z')-U(z)}\,\mathrm{d}z', \tag{4.7}$$

$$\epsilon_L = -\frac{\mathrm{i}\pi}{k}\frac{U''(z)\hat{u}^{\Lambda_1}_z(z;\,z)}{U'(z)}. \tag{4.8}$$

Provided there are no singularities, (4.6) implies that an arbitrary initial $\hat{w}_{y'}$ field may be expressed as a superposition of the Λ_1 CS modes. As will be seen in § 4.3, the expression for the amplitude distribution only becomes singular in the presence of discrete modes. For non-inflectional shearing flows, (4.6) is therefore equivalent to the Λ_1 modes forming a complete basis for $\hat{w}_{y',k}$ perturbations.

It is important to note that, although the solution via the Riemann–Hilbert problem achieves the formal inversion, thereby expressing the amplitude distribution of the CS modes in terms of the initial vorticity field, the explicit analytical forms for the individual Λ_1 eigenmodes (that is, $\hat{u}^{\Lambda_1}_z$ in (4.6)–(4.8)) will, for a general velocity profile, require a numerical solution. As shown by Balmforth & Morrison (1995), in the context of 2D perturbations, this may be accomplished in the present case by writing the velocity components $\hat{u}_{z,k}$ and $\hat{u}_{x',k}$ in terms of a scalar streamfunction (since $\hat{u}_{y',k}$ does not depend on the coordinate along $\boldsymbol{k}$). The streamfunction then satisfies a Fredholm integral equation of the second kind rather than the singular Cauchy integral equation above (a Fredholm equation of the first kind results for exceptional modes with zero net y' vorticity). For Couette flow, of course, the perturbation velocity fields are available in closed form. An approximate analytical inversion may be achieved, to $O(U'')$, when the curvature of the base-state velocity profile is small (Kelbert & Sazonov 1996).

Since each of the Λ_1 modes has an associated $\hat{u}_{y',k}(z)$ given by (3.10), the Λ_1 superposition needed to reproduce $\hat{w}_{y',k}(z,\,0)$ would also generate a $\hat{u}_{y'}$ contribution given by $\int_{-1}^{1} A^{\Lambda_1}(z')\hat{u}^{\Lambda_1}_{y'}(z;\,z')\,\mathrm{d}z'$ at the initial instant. This, of course, will not in general coincide with the initial $\hat{u}_{y',k}$ field given by $\mathscr{Q}_2(z)$. Thus, the superposition

of the Λ_2 modes needs to account for the difference between the $\mathscr{Q}_2(z)$ and that corresponding to the Λ_1 superposition above. One may write

$$\begin{aligned}\mathscr{Q}_2(z) &= \int_{-1}^{1} A^{\Lambda_1}(z')\hat{u}^{\Lambda_1}_{y',k}(z;\,z')\,\mathrm{d}z' + \int_{-1}^{1} A^{\Lambda_2}(z')\hat{u}^{\Lambda_2}_{y',k}(z;\,z')\,\mathrm{d}z',\\ &= \frac{U'(z)k_y}{\mathrm{i}kk_x}\,\mathcal{P}\int_{-1}^{1}\frac{A^{\Lambda_1}(z')\hat{u}^{\Lambda_1}_{z,k}(z;\,z')}{U(z)-U(z')}\,\mathrm{d}z' + A^{\Lambda_2}(z)\,\Sigma_2,\end{aligned} \tag{4.9}$$

where we have used the expression for $\hat{u}^{\Lambda_1}_{y',k}(z;\,z')$ from (3.10), and the fact that $\hat{u}^{\Lambda_2}_{y',k}(z;\,z')$ is just a delta function. The latter fact ensures that any initial $\hat{u}_{y'}$ field may trivially be represented as a superposition of the Λ_2 modes, since this merely amounts to the identity $f(z)=\int\delta(z-z')f(z')\,\mathrm{d}z'$ for an arbitrary function f. Thus,

$$A^{\Lambda_2}(z) = \frac{1}{\Sigma_2}\left[\mathscr{Q}_2(z) - \frac{U'(z)k_y}{\mathrm{i}kk_x}\,\mathcal{P}\int_{-1}^{1}\frac{A^{\Lambda_1}(z')\hat{u}^{\Lambda_1}_{z,k}(z;\,z')}{U(z)-U(z')}\,\mathrm{d}z'\right], \tag{4.10}$$

where $A^{\Lambda_1}(z)$ is known from (4.6). Combining (4.9) and (4.10), and accounting for the convection of the Λ_2 modes with the base-state velocities at the individual critical levels, we have the following expression for the arbitrary time evolution of $\hat{u}_{y',k}(z,\,t)$:

$$\hat{u}_{y',k}(z,\,t) = \mathscr{Q}_2(z)\,\mathrm{e}^{-\mathrm{i}k_xU(z)t} + \frac{U'(z)k_y}{\mathrm{i}kk_x}\int_{-1}^{1}A^{\Lambda_1}(z')\hat{u}^{\Lambda_1}_{z,k}(z;\,z')\frac{\mathrm{e}^{-\mathrm{i}k_xU(z')t}-\mathrm{e}^{-\mathrm{i}k_xU(z)t}}{U(z)-U(z')}\,\mathrm{d}z'. \tag{4.11}$$

Provided A^{Λ_1} given by (4.6) is non-singular, so is A^{Λ_2} as given by (4.10), and a combination of the Λ_1 and Λ_2 CS mode families then forms a complete basis for an arbitrary initial combination of the $\hat{w}_{y',k}$ and $\hat{u}_{y',k}$ fields. Since all other perturbation fields associated with a given Fourier mode may be expressed in terms of $\hat{w}_{y',k}$ and $\hat{u}_{y',k}$, and non-wave-like disturbances may be incorporated via the Fourier integral in (4.2), a combination of the Λ_1 and Λ_2 CS mode families is complete for non-inflectional shearing flows.

Equation (4.4) with $\hat{w}^{\Lambda_1}_{y',k}$ replaced by $\hat{u}^{\Lambda_1}_{z,k}$, together with (4.11), yield the modal superposition for a single Fourier mode with wavevector $\boldsymbol{k}$. One may now use (4.2) to obtain a superposition that underlies an arbitrary initial velocity field. To do this, (4.2) is rewritten in the form

$$\begin{aligned}\boldsymbol{u}(\boldsymbol{x},\,t) &= \int_{-\infty}^{\infty}\int_{-\infty}^{\infty}\mathrm{d}k_x\,\mathrm{d}k_y\,\mathrm{e}^{\mathrm{i}(k_xx+k_yy)}[\{\hat{\boldsymbol{x}}\mathrm{i}k^{-1}\cos\psi\,\mathrm{D}-\hat{\boldsymbol{y}}\mathrm{i}k^{-1}\sin\psi\,\mathrm{D}+\hat{\boldsymbol{z}}\}\hat{u}_{z,k}(z,\,t)\\ &\quad+\{\hat{\boldsymbol{x}}\sin\psi+\hat{\boldsymbol{y}}\cos\psi\}\hat{u}_{y',k}(z,\,t)],\end{aligned} \tag{4.12}$$

where $\hat{u}_{z,k}(z,\,t)$ and $\hat{u}_{y',k}(z,\,t)$ may be expressed as a superposition over the Λ_i modes ($i=1,\,2$). On using (4.4) written in terms of $\hat{u}^{\Lambda_1}_{z,k}$ and (4.11), one obtains the arbitrary time evolution in terms of the flow-aligned components of the initial perturbation velocity field:

$$\begin{aligned}\boldsymbol{u}(\boldsymbol{x},\,t) &= \int_{-\infty}^{\infty}\int_{-\infty}^{\infty}\mathrm{d}k_x\,\mathrm{d}k_y\,\mathrm{e}^{\mathrm{i}(k_xx+k_yy)}\\ &\quad\times\left[\{\hat{\boldsymbol{x}}\mathrm{i}k^{-1}\cos\psi\,\mathrm{D}-\hat{\boldsymbol{y}}\mathrm{i}k^{-1}\sin\psi\,\mathrm{D}+\hat{\boldsymbol{z}}\}\int_{-1}^{1}A^{\Lambda_1}(z')\hat{u}^{\Lambda_1}_{z,k}(z;\,z')\,\mathrm{e}^{-\mathrm{i}k_xU(z')t}\,\mathrm{d}z'\right.\end{aligned}$$

$$+\{\hat{\boldsymbol{x}}\sin\psi+\hat{\boldsymbol{y}}\cos\psi\}\Big\{[\hat{u}_{x,k}(z,0)\sin\psi+\hat{u}_{y,k}(z,0)\cos\psi]\,\mathrm{e}^{-\mathrm{i}k_xU(z)t}$$
$$-\frac{U'(z)k_y}{\mathrm{i}kk_x}\int_{-1}^{1}A^{\Lambda_1}(z')\hat{u}^{\Lambda_1}_{z,k}(z;z')\frac{\mathrm{e}^{-\mathrm{i}k_xU(z')t}-\mathrm{e}^{-\mathrm{i}k_xU(z)t}}{U(z)-U(z')}\,\mathrm{d}z'\Big\}\Big]. \tag{4.13}$$

Here, from (4.6), $A^{\Lambda_1}(z)$ may be expressed in terms of the initial perturbation field as:

$$A^{\Lambda_1}(z) = \frac{1}{\epsilon_R^2+\epsilon_L^2}\Bigg[\epsilon_R\left(\frac{\mathrm{i}}{k}(\mathrm{D}^2-k^2)\right)\hat{u}_{z,k}(z,0)$$
$$-\frac{\epsilon_L U'}{u^{\Lambda_1}_z(z;z)}\,\mathcal{P}\int_{-1}^{1}\frac{u^{\Lambda_1}_z(z;z')\left(\frac{\mathrm{i}}{k}(\mathrm{D}^2-k^2)\right)\hat{u}_{z,k}(z',0)}{U(z')-U(z)}\,\mathrm{d}z'\Bigg], \tag{4.14}$$

with ϵ_R and ϵ_L being given by (4.7) and (4.8). It is worth noting that $\psi = \tan^{-1}(k_y/k_x)$ in (4.13), and thus is not a constant since the singular-mode superposition corresponding to each elementary Fourier wave is constructed in a different coordinate system. Finally, the fact that the Λ_2 velocity field is a delta function (see (3.11)) may be used to rewrite (4.13) formally as the following superposition of separate terms involving the Λ_1 and Λ_2 modes:

$$\boldsymbol{u}(\boldsymbol{x},t) = \int_{-\infty}^{\infty}\int_{-\infty}^{\infty}\mathrm{d}k_x\,\mathrm{d}k_y\,\mathrm{e}^{\mathrm{i}(k_xx+k_yy)}$$
$$\times\Bigg[\int_{-1}^{1}A^{\Lambda_1}(z')\Bigg[\mathrm{e}^{-\mathrm{i}k_xU(z')t}\{\hat{\boldsymbol{x}}\mathrm{i}k^{-1}\cos\psi\,\mathrm{D}-\hat{\boldsymbol{y}}\mathrm{i}k^{-1}\sin\psi\,\mathrm{D}+\hat{\boldsymbol{z}}\}$$
$$-\frac{U'(z)k_y}{\mathrm{i}kk_x}\,\frac{\mathrm{e}^{-\mathrm{i}k_xU(z')t}-\mathrm{e}^{-\mathrm{i}k_xU(z)t}}{U(z)-U(z')}\{\hat{\boldsymbol{x}}\sin\psi+\hat{\boldsymbol{y}}\cos\psi\}\Bigg]\hat{u}^{\Lambda_1}_{z,k}(z;z')\,\mathrm{d}z'$$
$$+\frac{1}{\Sigma_2}\int_{-1}^{1}\{\hat{\boldsymbol{x}}\sin\psi+\hat{\boldsymbol{y}}\cos\psi\}[\hat{u}_{x,k}(z',0)\sin\psi+\hat{u}_{y,k}(z',0)\cos\psi]$$
$$\times\,\mathrm{e}^{-\mathrm{i}k_xU(z')t}\hat{u}^{\Lambda_2}_{y',k}(z;z')\,\mathrm{d}z'\Bigg], \tag{4.15}$$

with A^{Λ_1} being given by (4.14), and $u^{\Lambda_1}_{z,k}$ and $u^{\Lambda_2}_{y',k}$ being given by (3.9) and (3.11), respectively. The initial Fourier amplitudes, $\hat{\boldsymbol{u}}_k(z,0)$, used in (4.15) and (4.14), may be obtained from the following partial transform of the initial perturbation velocity field: $(1/(2\pi)^2)\int\mathrm{d}x\,\mathrm{d}y\,\mathrm{e}^{-\mathrm{i}(k_xx+k_yy)}\boldsymbol{u}(\boldsymbol{x},0)$.

For 2D perturbations, with $\psi=0$, (4.15) takes the much simpler form:

$$\boldsymbol{u}(\boldsymbol{x},t) = \int_{-\infty}^{\infty}\mathrm{d}k_x\,\mathrm{e}^{\mathrm{i}k_xx}\Bigg[\int_{-1}^{1}A^{\Lambda_1}(z')\,\mathrm{e}^{-\mathrm{i}k_xU(z')t}(\hat{\boldsymbol{x}}\mathrm{i}k^{-1}\mathrm{D}+\hat{\boldsymbol{z}})\hat{u}^{\Lambda_1}_{z,k_x}(z;z')\,\mathrm{d}z'$$
$$+\frac{\hat{\boldsymbol{y}}}{\Sigma_2}\int_{-1}^{1}\hat{u}_{y,k_x}(z',0)\,\mathrm{e}^{-\mathrm{i}k_xU(z')t}\hat{u}^{\Lambda_2}_{y,k_x}(z;z')\,\mathrm{d}z'\Bigg]. \tag{4.16}$$

Here the k_y integral in (4.15) has been eliminated, and the notation in (4.16) accounts for the coincidence of the flow-aligned and wavevector-aligned coordinate systems. Note that the individual velocity eigenfunctions remain unaltered in form (except for k being replaced by k_x), and A^{Λ_1} is still given by (4.14) with k replaced by k_x. The modal superposition in (4.16) degenerates into two decoupled contributions, and this may be explicitly seen by writing down the separate integral superpositions corresponding to the normal and spanwise components of the perturbation velocity field (the first term in the operator, $(\hat{\boldsymbol{x}}\mathrm{i}k^{-1}\mathrm{D}+\hat{\boldsymbol{z}})$, merely reflects the incompressibility constraint that relates the x and z components of the perturbation field). From (4.16), we have

$$u_z(\boldsymbol{x},t) = \int_{-\infty}^{\infty} \mathrm{d}k_x\, \mathrm{e}^{\mathrm{i}k_x x} \int_{-1}^{1} A^{\Lambda_1}(z')\, \mathrm{e}^{-\mathrm{i}k_x U(z')t} \hat{u}^{\Lambda_1}_{z,k}(z;z')\, \mathrm{d}z', \tag{4.17}$$

$$u_y(\boldsymbol{x},t) = \frac{1}{\Sigma_2} \int_{-1}^{1} \hat{u}_{y,k}(z',0)\, \mathrm{e}^{-\mathrm{i}k_x U(z')t} \hat{u}^{\Lambda_2}_{y,k_x}(z;z')\, \mathrm{d}z'. \tag{4.18}$$

The expression (4.18) merely represents a spanwise perturbation, convected by the shear flow, and independent of the dynamics of perturbations in the plane of shear. Operating (4.17) with $(\mathrm{i}/k)(\mathrm{D}^2-k^2)$ on both sides leads to an equivalent superposition in terms of the $\hat{w}_y^{\Lambda_1}(z,z')$ vorticity field that is already known (Balmforth & Morrison 1995). For Couette flow, $\hat{w}_y^{\Lambda_1}(z,z') \propto \delta(z-z')$, and (4.17) takes the same form as (4.18) since both the spanwise vorticity and velocity fields are merely convected by the flow in this limit. The physical interpretation of the Orr mechanism, based on this $\hat{w}_y^{\Lambda_1}$ superposition, was discussed in the introduction (see figure 2).

4.2. *Transient growth for a 'roll' initial condition*

Considering again the superposition for a fixed $\boldsymbol{k}$, we note that, for a vanishingly small streamwise wavenumber, (4.11) reduces to

$$\begin{aligned}
\hat{u}_{y',k}(z,t) &= \hat{u}_{y',k}(z,0) - U'(z)\left[t\hat{u}_{z,k}(z,0)\right.\\
&\quad \left. - \frac{\mathrm{i}k_x t^2}{2}\int_{-1}^{1} A^{\Lambda_1}(z')\hat{u}^{\Lambda_1}_{z,k}(z;z')\{U(z')+U(z)\}\,\mathrm{d}z' + O(k_x^2 t^3)\right],\\
&= \hat{u}_{y',k}(z,0) - U'(z)t\left[\hat{u}_{z,k}(z,0)\right.\\
&\quad \left. - \frac{\mathrm{i}k_x t}{2}\left\{\hat{u}_{z,k}(z,0)U(z) + \int_{-1}^{1} A^{\Lambda_1}(z')\hat{u}^{\Lambda_1}_{z,k}(z;z')U(z')\,\mathrm{d}z'\right\} + O(k_x t)^2\right],
\end{aligned} \tag{4.19}$$

where we have used $k_y = -k(\psi = -\pi/2)$, and that

$$\hat{u}_{z,k}(z,0) = \int_{-1}^{1} A^{\Lambda_1}(z')\hat{u}^{\Lambda_1}_{z,k}(z;z')\,\mathrm{d}z'. \tag{4.20}$$

Thus, the relevant (dimensionless) small parameter in (4.19) is $k_x\bar{U}_c t$, $\bar{U}_c$ being a characteristic velocity scale of the base-state profile, and not k_x alone. The expression

(4.19) evidently predicts an algebraic growth over a time scale $t \ll O(k_x \bar{U}_c)^{-1}$. For times of $O(k_x \bar{U}_c)^{-1}$, however, all terms in the series expansion within brackets become comparable and the resulting mutual cancellation leads to a saturation of the initial algebraic growth. Physically, this is indicative of differential convection of the perturbation by the base-state shear, leading to decoherence (phase mixing) for long times. For $k_x = 0$, that is, a streamwise-uniform initial condition, the role of shear in phase mixing becomes redundant and the algebraic growth persists for all times, with

$$\hat{u}_{y',k}(z, t) = \hat{u}_{x,k}(z, t) = \hat{u}_{x,k}(z, 0) - U'(z) t \, \hat{u}_{z,k}(z, 0), \tag{4.21}$$

where we have used that the y'-axis coincides with the flow direction (x) for a streamwise-uniform perturbation. The expression (4.21) is the algebraic instability for a streamwise-uniform Fourier mode ($k = k_y$) where an upward normal velocity perturbation associated with a 'roll' Fourier mode carries slow-moving fluid to higher z locations, creating a negative $u_{y'}$ perturbation. An inverse Fourier transform leads one precisely to the relation obtained by Ellingsen & Palm (1975). Thus, the algebraic instability for 3D disturbances in shear flows is contained in the modal superposition of the Λ_i eigenfunctions.

In order to obtain a clearer physical picture of the instability, we consider the manner in which the modal superposition in (4.11) reproduces a 'roll' initial condition with the velocity field restricted to the (x', z) plane. We further simplify the physical picture by restricting ourselves to Couette flow with $U''(z) = 0$, in which case the $w_{y'}$ component of a Λ_1 mode reduces to a delta function. There is no real loss of generality since, as is evident from (4.21), it is the velocity gradient (U') and not the vorticity gradient ($\propto U''$) that is responsible for the algebraic instability. The latter is, of course, crucial to the existence of unstable discrete modes that are analysed briefly in the next subsection. The 2D nature of the roll implies that the only non-zero vorticity component in the initial condition is $w_{y'}(z, 0)$. This initial field may readily be formed by a stack of Λ_1 CS modes. The amplitude of a particular eigenmode, this being the strength of the $w_{y'}$ vortex sheet, is proportional to $w_{y'}(z, 0)$ at the z corresponding to the location of the $w_{y'}$ vortex sheet (which, of course, is the critical level of the particular mode considered). Note that, except for 2D perturbations, the vorticity field associated with a Λ_1 mode remains 3D, and the term 'vortex sheet' here refers only to the delta function in $w_{y'}$. Now, for any $\boldsymbol{k}$ that has a spanwise projection, each of the Λ_1 modes also has a PV-singular $u_{y'}$ field not present in the roll initial condition. This $u_{y'}$ field generated by the Λ_1 superposition must therefore be precisely cancelled out by an appropriate superposition of Squire jets at the initial instant. Since the jet refers to a delta function $u_{y'}$ field, the amplitude of each Squire jet in this superposition must again be equal in magnitude, but opposite in sign, to the local $u_{y'}$ induced by the Λ_1 superposition. The precise cancellation in $u_{y'}$ can only happen at $t = 0$, however. For subsequent times, the differential convection of the CS modes by the base-state shear undoes the cancellation, leading to a growing $u_{y'}$, that is, a temporally growing streak. For any finite k_x, eventual decoherence in phase will terminate the initial algebraic growth but, as the initial condition approaches streamwise uniformity ($k_x \to 0$), this phase mixing becomes infinitely slow. Figure 4 illustrates the above picture for the case of an initial roll with $k_x = 0$, and whose velocity field in the $(x', z) \equiv (x, z)$ plane is that associated with a single Λ_1 mode. The amplitude distribution of the Λ_2 modes therefore follows an envelope that has a principal value singularity at the critical level of the Λ_1 mode, and a growing streak results in this case from the differential convection of the Squire jets alone. In summary, the 'lift-up' effect, in a modal approach, may be interpreted as resulting

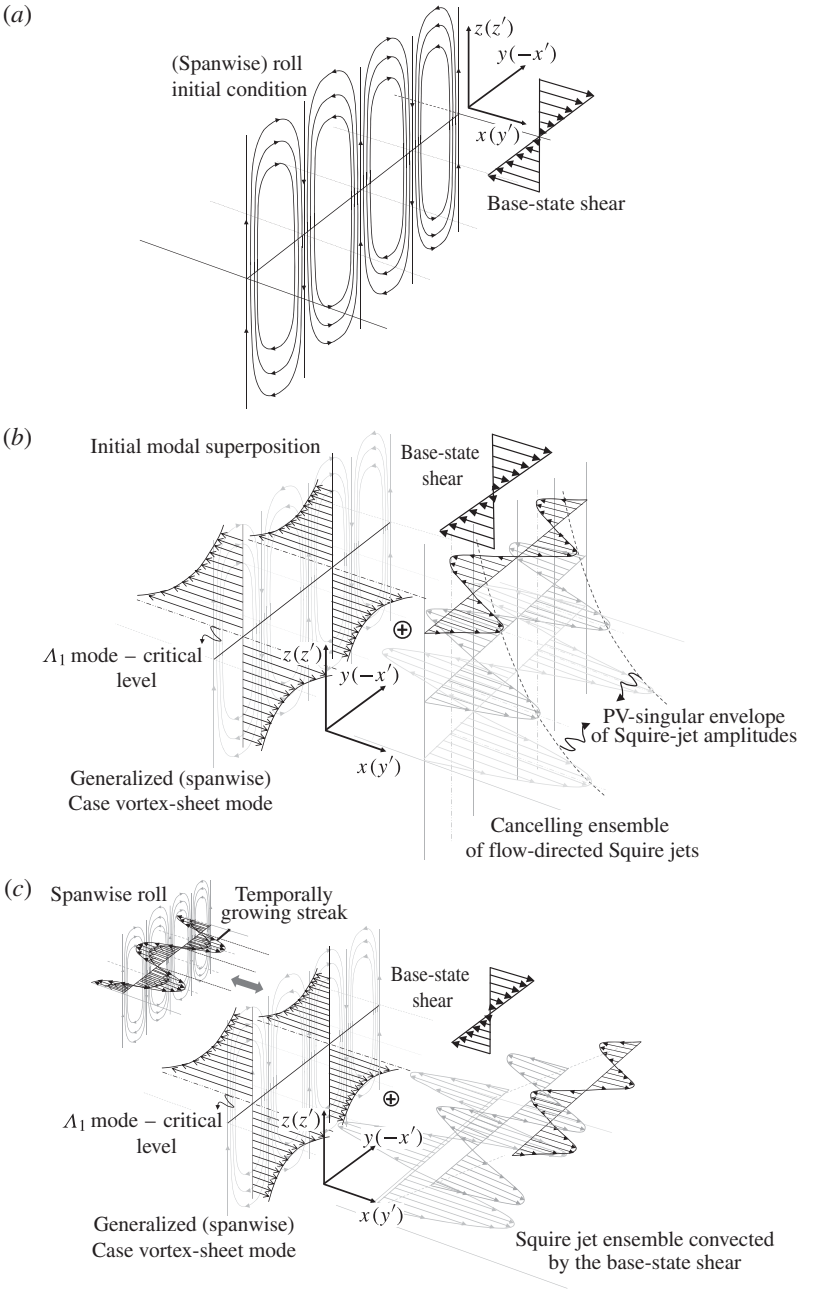

FIGURE 4. An initial roll evolving, via a superposition of a single Case vortex sheet and a Squire jet ensemble, in a reference frame that translates with the base-state flow velocity at the critical level of the Case vortex sheet. (*a*) Spanwise-oriented roll initial condition corresponding to the (partial) velocity field of a single Case mode. (*b*) Initial superposition of a single Case mode and the ensemble of Squire jets that effects a precise cancellation of the streamwise velocity component. (*c*) Dephasing of Squire jets due to differential convection by the base-state shear flow, leading to a growing streak. Both the non-modal (upper left) and modal interpretations are depicted.

from the evolution of a flow-aligned cancelling superposition of the Λ_1 vortex-sheet modes and the corresponding ensemble of Squire jets at the initial instant. Finally, we note that (4.21) is valid even for nonlinear velocity profiles with a non-trivial base-state vorticity gradient. The argument above also holds in these cases, except that the details of the superposition become complicated. For instance, the amplitude $A^{\Lambda_1}(z)$, instead of obeying a trivial algebraic relation, $A^{\Lambda_1}(z')\Sigma_1 = \mathscr{Q}_1$, as for Couette flow, is now determined by an integral equation instead (see (4.6)).

4.3. *Inclusion of discrete modes*

The expression (4.13) for the evolution of a general initial condition in terms of the Λ_1 and Λ_2 families can be generalized to the case of inflectional velocity profiles by accommodating additional discrete modes associated with each inflection point. This may be done using the original formulation of Case (1959) in the plasma physics context, and has already been adapted by Balmforth & Morrison (1995) and Roy & Subramanian (2014) in the hydrodynamical context. We will therefore be brief here. As already mentioned, the expression (4.14) for $A^{\Lambda_1}(z)$ is obtained as the solution of a Riemann–Hilbert problem, and is, in fact, the limiting form (on the real axis) of the following relation in the complex plane:

$$\Psi(z) = \frac{\chi(z)}{1 + 2\pi \mathrm{i}\Phi(z)}, \tag{4.22}$$

where $z = z_R + \mathrm{i}z_I$ is now regarded as a complex variable, and where

$$\Psi(z) = \frac{1}{2\pi \mathrm{i}} \int_{-1}^{1} \frac{A^{\Lambda_1}(z')\hat{u}_z^{\Lambda_1}(z; z')}{U(z') - U(z)}\, \mathrm{d}z', \tag{4.23}$$

$$\Phi(z) = \frac{1}{2\pi \mathrm{i}} \left(\frac{-\mathrm{i}}{k\Sigma_1}\right) \int_{-1}^{1} \frac{U''(z')\hat{u}_z^{\Lambda_1}(z'; z)}{U(z') - U(z)}\, \mathrm{d}z' \tag{4.24}$$

and

$$\chi(z) = \frac{1}{2\pi \mathrm{i}} \left(\frac{1}{\Sigma_1}\right) \int_{-1}^{1} \frac{Q_1(z')\hat{u}_z^{\Lambda_1}(z; z')}{U(z') - U(z)}\, \mathrm{d}z' \tag{4.25}$$

are sectionally analytic functions in the complex plane with a branch cut along $z \epsilon (-1, 1)$. The expression (4.14) is valid when the only singularity of $\Psi(z)$ is the aforementioned branch cut. This is, however, no longer true when there exist points $z = c_n$ in the complex plane, in the strip $-1 < z_R < 1$ (on account of the Howard semi-circle theorem; see Drazin & Reid (1981)), where $1 + 2\pi \mathrm{i}\Phi(c_n) = 0$. Using the definition of $\Phi(z)$ above, this relation may be written as

$$1 - \frac{\mathrm{i}}{k\Sigma_1} \int_{-1}^{1} \frac{U''(z')\hat{u}_{z',k}^{\Lambda_1}(z; c_n)}{U(z') - c_n}\, \mathrm{d}z' = 0. \tag{4.26}$$

This is the dispersion relation for the discrete modes associated with the Rayleigh operator. The normalization based on the total $\hat{w}_{y'}$ field implies that $\hat{u}_{z',k}^{\Lambda_1}$ is purely imaginary, and the coefficients in (4.26) are therefore real-valued, allowing for both c_n and c_n^* as solutions; here '$*$' denotes a complex conjugate. The corresponding eigenfunctions bear a similar relation. In other words, as is well known, the inviscid

discrete modes occur in conjugate pairs. In the presence of discrete modes, one may use the modified function

$$\chi_m(z)\frac{1}{2\pi\mathrm{i}}\left(\frac{1}{\Sigma_1}\right)\int_{-1}^{1}\frac{Q_1(z')\hat{u}_z^{\Lambda_1}(z;z')-\sum_n[A_n\hat{u}_{z,k}^{\Lambda_1}(z;c_n)+A_n^*\hat{u}_{z,k}^{\Lambda_1}(z;c_n^*)]}{U(z')-U(z)}\,\mathrm{d}z', \tag{4.27}$$

where $\hat{u}_{z,k}^{\Lambda_1}(z;c_n)$ and $\hat{u}_{z,k}^{\Lambda_1}(z;c_n^*)$ are the discrete mode eigenfunctions, and A_n and A_n^* are their amplitudes. The summation with respect to n is over all pairs of discrete modes. The discrete modal amplitudes are determined by enforcing the analyticity of $\Psi(z)$, now defined by a relation similar to (4.22) but involving $\chi_m(z)$, at the points $z=c_n$ and $z=c_n^*$. The resulting expressions for $u_{z,k}(z,t)$ and $u_{y',k}(z,t)$ are given by

$$\begin{aligned}\hat{w}_{y',k}(z,t) &= \sum_n[A_n\hat{w}_{z,k}^{\Lambda_1}(z;c_n)\,\mathrm{e}^{-\mathrm{i}k_xc_nt}+A_n^*\hat{w}_{z,k}^{\Lambda_1}(z;c_n^*)\,\mathrm{e}^{-\mathrm{i}k_xc_n^*t}]\\ &\quad+\int_{-1}^{1}A^{\Lambda_1}(z')\hat{w}_{z,k}^{\Lambda_1}(z;z')\,\mathrm{e}^{-\mathrm{i}k_xU(z')t}\,\mathrm{d}z', \qquad (4.28)\\ \hat{u}_{y',k}(z,t) &= Q_2(z)\,\mathrm{e}^{-\mathrm{i}k_xU(z)t}+\frac{U'(z)k_y}{\mathrm{i}kk_x}\int_{-1}^{1}A^{\Lambda_1}(z')\hat{u}_{z,k}^{\Lambda_1}(z;z')\frac{\mathrm{e}^{-\mathrm{i}k_xU(z')t}-\mathrm{e}^{-\mathrm{i}k_xU(z)t}}{U(z)-U(z')}\,\mathrm{d}z'\\ &\quad+\frac{U'(z)k_y}{\mathrm{i}kk_x}\sum_n\left[A_n\hat{u}_{z,k}^{\Lambda_1}(z;c_n)\frac{\mathrm{e}^{-\mathrm{i}k_xc_nt}-\mathrm{e}^{-\mathrm{i}k_xU(z)t}}{U(z)-c_n}\right.\\ &\quad\left.+A_n^*\hat{u}_{z,k}^{\Lambda_1}(z;c_n^*)\frac{\mathrm{e}^{-\mathrm{i}k_xc_n^*t}-\mathrm{e}^{-\mathrm{i}k_xU(z)t}}{U(z)-c_n^*}\right], \qquad (4.29)\end{aligned}$$

where $A^{\Lambda_1}(z)$ is now given by

$$A^{\Lambda_1}(z) = \frac{1}{\epsilon_R^2+\epsilon_L^2}\left[\epsilon_R\mathscr{R}_1-\frac{\epsilon_LU'}{u_z^{\Lambda_1}(z;z)}\,\mathcal{P}\int_{-1}^{1}\frac{\hat{u}_{z,k}^{\Lambda_1}(z;z')\mathscr{R}_1(z')}{U(z')-U(z)}\,\mathrm{d}z'\right], \tag{4.30}$$

$$\mathscr{R}_1(z) = \mathscr{Q}_1(z)-\frac{\mathrm{i}}{k}(\mathrm{D}^2-k^2)\sum_n[A_n\hat{u}_{z,k}(z;c_n)+A_n^*\hat{u}_{z,k}(z;c_n^*)], \tag{4.31}$$

$$A_n = \frac{\displaystyle\int_{-1}^{1}\frac{\mathscr{Q}_1(z)u_{zn}(z;c_n)}{U(z)-c_n}\,\mathrm{d}z}{\displaystyle\frac{\mathrm{i}}{k}\int_{-1}^{1}\left\{\frac{\hat{u}_{z,k}(z;c_n)}{U(z)-c_n}\right\}^2U''(z)\,\mathrm{d}z}, \tag{4.32}$$

with ϵ_R and ϵ_L being given by (4.7) and (4.8) and $\mathscr{Q}_1(z)=(\mathrm{i}/k)(\mathrm{D}^2-k^2)\hat{u}_{z,k}(z,0)$ as before. When compared with (4.6) for a non-inflectional profile (with a purely continuous spectrum), (4.30) highlights the removal, from the initial condition, of its projection onto the discrete modes. Note that the discrete spectrum in the inviscid limit is associated with the Rayleigh operator alone, and as evident from the expression for (4.29) for the $\hat{u}_y'$ field, the inviscid Squire spectrum remains purely continuous regardless of inflection points.

5. The relation between the inviscid and viscous modal superpositions

The earlier sections have dealt with an inviscid modal interpretation of the lift-up effect. For any finite Re, the dynamics of the linearized perturbations is governed by the Orr–Sommerfeld and Squire equations, which, in non-dimensional form, are given by

$$\left[\left(\frac{\partial}{\partial t}+U\frac{\partial}{\partial x}-\frac{1}{Re}\nabla^2\right)\nabla^2-U''\frac{\partial}{\partial x}\right]u_z=0, \tag{5.1}$$

$$\left[\frac{\partial}{\partial t}+U\frac{\partial}{\partial x}-\frac{1}{Re}\nabla^2\right]w_z=-U'\frac{\partial u_z}{\partial y}. \tag{5.2}$$

Written in normal-mode form, the homogeneous solution of (5.1), together with the forced solution of (5.2), is termed an Orr–Sommerfeld (OS) eigenmode, while the homogeneous solution of (5.2) with $u_z=0$ is termed a Squire eigenmode (Schmid & Henningson 2001). This is analogous to our classification of the inviscid eigenmodes, satisfying (2.3) and (2.4), in terms of the Λ_1 and Λ_2 families, but for the difference in the coordinate systems (space-fixed here as opposed to wavevector-aligned in § 2).

An explanation for the lift-up effect, based on the evolution of an initial cancelling superposition of the aforementioned viscous eigenmodes, appears in Schmid & Henningson (2001, pp. 106–107). We quote a brief passage from this description:

> Suppose that we expand an initial condition with zero normal vorticity. This will excite a number of Orr–Sommerfeld modes to represent the initial normal velocity. Each Orr–Sommerfeld mode has an associated particular normal vorticity, which now needs to be cancelled by an appropriate combination of Squire modes. Thus both Orr–Sommerfeld and Squire modes are excited by an initial condition of zero normal vorticity. As the disturbance evolves downstream, each mode evolves in time according to its eigenvalue. Because the phase speeds and decay rates are different the modes will propagate apart and the cancellation that was enforced for $t=0$ will not persist. Consequently, the disturbance will experience transient growth in the normal vorticity component.

Unlike the inviscid problem, the viscous eigenmodes involved in such a superposition, and the viscous spectrum itself, are not known in closed form owing to the analytical intractability of the OS equation. Nevertheless, it is worth examining the relation between the inviscid and viscous modal superpositions. A pertinent question is whether there is a one-to-one correspondence between the inviscid eigenmodes and the viscous eigenmodes for large Re involved in the superposition that reproduces a roll initial condition. As will be shown below, this is not so, at least in the example considered, that of Couette flow, owing to fundamental differences between the inviscid spectrum and the large-Re viscous spectrum.

In what follows, we examine the evolution of a given initial condition, via inviscid singular eigenfunctions, and as a superposition of viscous discrete modes in the limit of a vanishingly small viscosity, for the analytically soluble example of Couette flow. The constancy of the base-state vorticity makes it convenient to formulate the linearized dynamics in Couette flow in terms of an appropriate component of the perturbation vorticity field that satisfies the advection–diffusion equation. If ϕ is the particular vorticity component, we have

$$\frac{\partial\phi}{\partial t}+U(z)\frac{\partial\phi}{\partial x}=\nu\nabla^2\phi, \tag{5.3}$$

where $U(z) = \dot{\gamma} z$, $\dot{\gamma}$ being the shear rate (taken to be unity in earlier sections). Assuming a Fourier mode of the form $\phi(\boldsymbol{x}, t) = \hat{\phi}(z, t)\, \mathrm{e}^{\mathrm{i}(k_x x + k_y y)}$, and using k^{-1} and $(\dot{\gamma} \cos \psi)^{-1}$ as characteristic length and time scales (the angle ψ is defined in figure 3), the non-dimensional equation in modal form is

$$\frac{\partial \hat{\phi}}{\partial t} + \mathrm{i}z\hat{\phi} = \frac{1}{Re}\left(\frac{\partial^2 \hat{\phi}}{\partial z^2} - \hat{\phi}\right), \tag{5.4}$$

where $Re = \dot{\gamma} \cos \psi\, (\nu k^2)^{-1}$. For the Squire equation, $\hat{\phi} = \hat{w}_z$, with homogeneous boundary conditions. For the OS equation, $\hat{\phi} \propto \hat{w}_{y'}$, with homogeneous boundary conditions for the normal and tangential velocities given by $(\partial^2/\partial z^2 - k^2)^{-1}\hat{\phi}$ and $(\partial/\partial z)(\partial^2/\partial z^2 - k^2)^{-1}\hat{\phi}$, respectively. We analyse, in turn, the relations between the inviscid spectra and the limiting forms of the viscous spectra for the Squire and OS operators. Finally, we consider streamwise-uniform disturbances ($\psi = \pm(\pi/2)$), which require separate consideration, since Re, as defined above, approaches zero, and the time scale must be modified to reflect the diffusive decay of the eigenmodes.

5.1. *Viscous spectrum of the Squire equation*

For $Re = \infty$, (5.4) supports an inviscid CS over the base-state range of velocities. A given eigenmode is convected with the local fluid velocity at $z = z_1$ (say), being of the form $\hat{\phi}(z, t) = \delta(z - z_1)\, \mathrm{e}^{-\mathrm{i}z_1 t}$. Physically, this infinitely localized vortical structure corresponds to a Squire jet. Viscosity, however, causes the width of the vorticity distribution to grow as $O(t/Re)^{1/2}$. The form of the finite-Re response, for any t, is given by the Green's function, $\mathcal{G}(z, t; z_1)$, of the advection–diffusion operator defined as

$$\frac{\partial \mathcal{G}}{\partial t} + \mathrm{i}z\mathcal{G} - \frac{1}{Re}\left(\frac{\partial^2 \mathcal{G}}{\partial z^2} - \mathcal{G}\right) = \delta(z - z_1)\delta(t), \tag{5.5}$$

which is readily solved to obtain

$$\mathcal{G}(z, t; z_1) = \sqrt{\frac{Re}{4\pi t}} \exp\left[-\frac{\mathrm{i}t(z + z_1)}{2} - \frac{t}{Re}\left(\frac{t^2}{12} + 1\right) - \frac{(z - z_1)^2 Re}{4t}\right], \tag{5.6}$$

for an unbounded domain. For a semi-infinite domain, the condition $\mathcal{G} = 0$ at $z = 0$ is satisfied by adding image vorticity of the opposite sign at $z = -z_1$ (Marcus & Press 1977). The effect of boundaries is, however, secondary in the arguments that follow, the focus being on the structure of the viscous eigenmodes outside wall boundary layers. Since (5.6) may be written in the form

$$\begin{aligned}\mathcal{G}(z, t; z_1) \;=\; & \sqrt{\frac{Re}{4\pi t}} \exp\left[-\frac{t}{Re}\left(\frac{t^2}{12} + 1\right)\right] \\ & \times \int_{-\infty}^{\infty} \exp\left[\frac{\mathrm{i}t(z' - z_1)}{2} - \frac{(z' - z_1)^2 Re}{4t}\right] \delta(z - z')\, \mathrm{e}^{-\mathrm{i}z' t}\, \mathrm{d}z',\end{aligned} \tag{5.7}$$

the finite-Re solution may be interpreted as a time-varying superposition of localized jets, the amplitude envelope of this superposition broadening as the square root of time. The most important point is the non-separable dependence on z and t, implying that (5.6) is not of a normal-mode form. That a non-modal viscous structure reduces to

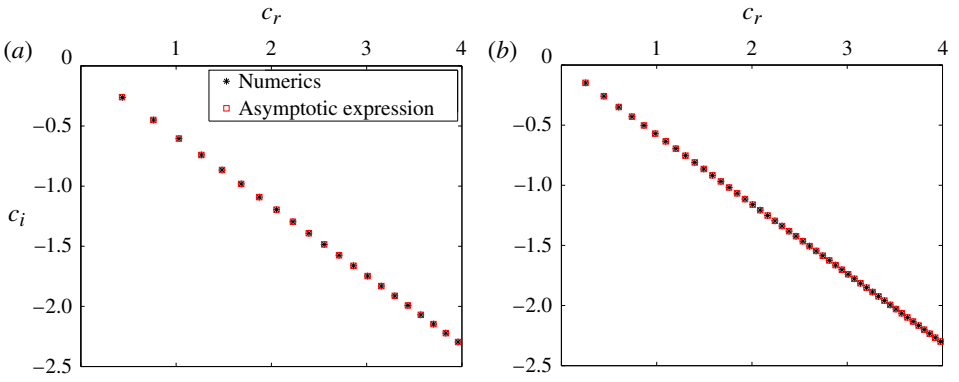

FIGURE 5. (Colour online) The viscous Squire spectrum for semi-infinite Couette flow ($U \propto z$ with $0 \leqslant z < \infty$) for (*a*) $Re = 100$ and (*b*) $Re = 500$: $*$, equation (5.9); $\square$, equation (5.10).

a single inviscid mode (a convected jet) in the limit $Re \to \infty$ highlights the non-trivial nature of the viscous–inviscid relation.

To characterize the viscous spectrum, we consider a solution of (5.4), in the normal-mode form $\hat{\phi}(z, t) = \Phi(z)\,\mathrm{e}^{-\mathrm{i}ct}$, where $\Phi(z)$ satisfies the following differential equation:

$$\frac{\mathrm{d}^2\Phi}{\mathrm{d}z^2} = \{\mathrm{i}Re(z - c) + 1\}\Phi. \tag{5.8}$$

This has solutions in terms of the two Airy functions $\mathrm{Ai}[(\mathrm{i}Re)^{1/3}\{z - c + (\mathrm{i}Re)^{-1}\}]$ and $\mathrm{Bi}[(\mathrm{i}Re)^{1/3}\{z - c + (\mathrm{i}Re)^{-1}\}]$. For purposes of simplicity, we consider a semi-infinite domain with the boundary conditions $\Phi(0) = 0$ and $\Phi(z) \to 0$ as $z \to \infty$. The latter condition implies that only Ai need be considered, and the viscous eigenvalues satisfy the relation $\mathrm{Ai}[(\mathrm{i}Re)^{1/3}\{-c + (\mathrm{i}Re)^{-1}\}] = 0$, being given by

$$c_n = -\frac{\mathrm{ai}_n}{(\mathrm{i}Re)^{1/3}} + \frac{1}{\mathrm{i}Re}, \tag{5.9}$$

where ai_n is the nth zero of $\mathrm{Ai}(z)$. The spectrum is evidently discrete. The asymptotic form of ai_n (Abramowitz & Stegun 1965) yields the following large-n approximation:

$$c_n \approx \left[\left\{\frac{3\pi(4n - 1)}{8}\right\}^2 \frac{1}{\mathrm{i}Re}\right]^{1/3} + \frac{1}{\mathrm{i}Re}. \tag{5.10}$$

Figure 5 shows the favourable comparison between the eigenvalues evaluated using (5.9) and (5.10) for $Re = 100$ and 500. With increasing Re, the spacing between the eigenvalues decreases, and a given eigenvalue (n fixed) approaches the boundary ($c = 0$). The latter arises because unbounded viscous Couette flow does not have normal modes with the only known solutions having a non-separable space–time dependence. Those that have a localized wavepacket-like character are given by (5.7), and the delocalized solutions are viscously decaying Kelvin modes (Farrell & Ioannou 1993). As a result, the normal modes in Couette flow with one or more boundaries are the so-called 'wall modes' (Schmid & Henningson 2001) with a structure that, for large Re, is localized in the vicinity of the boundary. The balance between

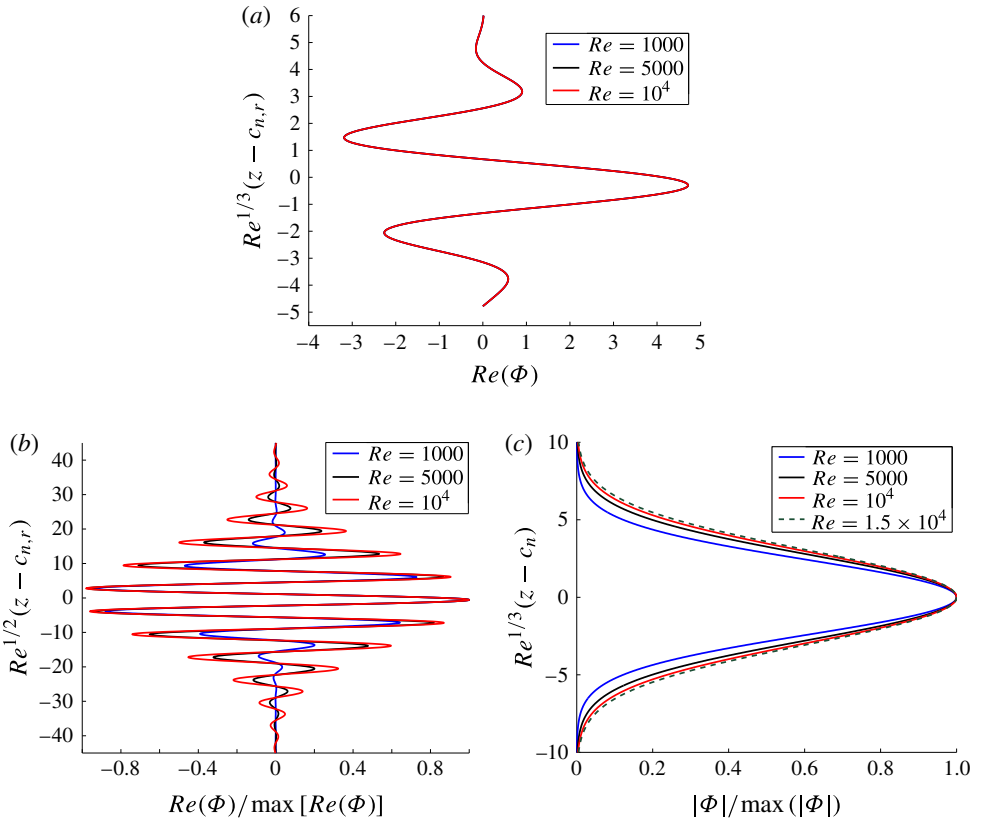

FIGURE 6. (Colour online) The structure of the Squire eigenmodes for various Re values. (a) The $O(Re^{-1/3})$ scaling for a weakly damped wall mode (Squire mode with $n = 3$). (b,c) Interior Squire modes that decay at an inviscid rate: (b) nth mode, $O(Re^{-1/2})$ scaling of oscillations; (c) nth mode, $O(Re^{-1/3})$ scaling of the envelope. For a value of Re, the interior mode is chosen with $n \sim Re^{1/2}$ to ensure that the eigenvalue remains $O(1)$ ($c_{n,r} = Re(c_n)$).

convection by shear and viscous diffusion implies that the spatial extent of this wall boundary layer is $[O(Re)^{-1/3}]$; see figure 6(a). More interestingly, as seen in figure 5, the spectra for large Re values increasingly lie on a single ray that emerges from the origin at an angle of $\pi/6$ with the real axis. This invariant ray is the limiting form of the viscous spectrum for $Re = \infty$, as is evident from the term of $O(Re^{-1/3})$ in (5.10) (Reddy, Schmid & Henningson 1993). While eigenvalues with a fixed n approach the origin with increasing Re, one can always find an eigenvalue, with a sufficiently large modal index ($n \sim O(Re^{1/2})$), that remains on the aforementioned ray at an $O(1)$ distance from the positive real axis (the inviscid CS). Physically, $c_i \sim O(1)$ implies that such an 'interior mode' decays at an inviscid rate. This may also be seen from the asymptotic form of the Airy function for large arguments given by $\mathrm{Ai}(\zeta) \approx \mathrm{e}^{-2\zeta^{3/2}/3}/(2\sqrt{\pi}\zeta^{1/4})$ ($|\arg\zeta| < \pi$) with $\zeta = (\mathrm{i}Re)^{1/3}(z - c_n)$ (Abramowitz & Stegun 1965). For large Re, and with z, $c_n \sim O(1)$, the above asymptote shows a separation between the $O(Re^{-1/3})$ length scale characterizing the extent of the wavepacket and the $O(Re^{-1/2})$ scale characterizing the oscillations within. The scale of the oscillations in a packet decreases with increasing Re in precisely such a manner

as to maintain an inviscid decay rate. The existence of two increasingly disparate scales in a large-Re viscous eigenfunction is illustrated in figure 6(b,c).

Having characterized the viscous modal solutions, one may now use the adjoint eigenfunctions of (5.8), and, proceeding along standard lines for an operator with a discrete spectrum (Stakgold 1968; Friedman 1990), arrive at the following representation of the delta function in terms of the direct and adjoint viscous modes:

$$\delta(z-z_1)=\sum_{n=1}^{\infty}\frac{(\mathrm{i}Re)^{1/3}\mathrm{Ai}\left[(\mathrm{i}Re)^{1/3}\left\{z_1-c_n+\dfrac{1}{\mathrm{i}Re}\right\}\right]}{\mathrm{Ai}'\left[(\mathrm{i}Re)^{1/3}\left\{-c_n+\dfrac{1}{\mathrm{i}Re}\right\}\right]^2}\mathrm{Ai}\left[(\mathrm{i}Re)^{1/3}\left\{z-c_n+\frac{1}{\mathrm{i}Re}\right\}\right]. \tag{5.11}$$

Physically, the above representation relates an inviscid Squire eigenmode, at the initial instant, to a linear superposition of the corresponding viscous discrete modes. The generalization of (5.11) to any finite time is given by

$$\mathcal{G}'(z,t;z_1)=\sum_{n=1}^{\infty}\frac{(\mathrm{i}Re)^{1/3}\mathrm{Ai}\left[(\mathrm{i}Re)^{1/3}\left\{z_1-c_n+\dfrac{1}{\mathrm{i}Re}\right\}\right]}{\mathrm{Ai}'\left[(\mathrm{i}Re)^{1/3}\left\{-c_n+\dfrac{1}{\mathrm{i}Re}\right\}\right]^2}\mathrm{Ai}\left[(\mathrm{i}Re)^{1/3}\left\{z-c_n+\frac{1}{\mathrm{i}Re}\right\}\right]\mathrm{e}^{-\mathrm{i}c_nt}. \tag{5.12}$$

The spatial extent of the viscous wavepacket in (5.12) is governed by $\mathrm{Ai}[(\mathrm{i}Re)^{1/3}\{z-c_n+1/(\mathrm{i}Re)\}]$, and the number of viscous modes included in the above summation therefore corresponds to the number of c_n in the interval where $(z_1-c_n)\sim O(Re^{-1/3})$. From (5.10), with $n\sim O(Re^{1/2})$, it may be shown that the eigenvalue spacing decreases as $Re^{-5/6}$, and thus, even as the spatial extent of the viscous wavepacket in (5.10) decreases with increasing Re, the number of viscous modes contributing to the wavepacket diverges as $Re^{1/2}$. The physical content of the modal superposition is better seen from (5.6), which emphasizes the slow viscous broadening of the initially localized jet. Note that, between (5.6) and (5.12), only the latter is constrained to vanish at $z=0$, but the difference between the two is exponentially small at the boundary for $Re\gg 1$ provided z_1 is $O(1)$.

In the interest of analytical simplicity, the above discussion has emphasized the relation between the viscous and inviscid spectra for Couette flow in a semi-infinite domain, in which case the large-Re Squire spectrum emerges from the origin as a single ray, at an angle $\theta=\pi/6$ with the real axis, extending to infinity (see figure 5). For bounded Couette flow, the spectrum is Y-shaped and there are now two symmetrical branches consisting of localized wall modes near either boundary (Schmid & Henningson 2001). The branches meet and continue downwards as a vertical stem, which consists of stationary eigenmodes given by a linear combination of the Airy functions of both kinds. Importantly, the Y-shaped locus itself is expected to remain invariant, with the junction remaining at an $O(1)$ distance from the real axis even as $Re\to\infty$; numerical evidence in this regard is available in Reddy *et al.* (1993, figures 9 and 10 therein). Thus, even as the eigenvalues rise up the stem, and onto the branches, approaching the boundaries for a fixed modal index n and increasing Re, there are always eigenvalues with n large enough (again of $O(Re^{1/2})$)

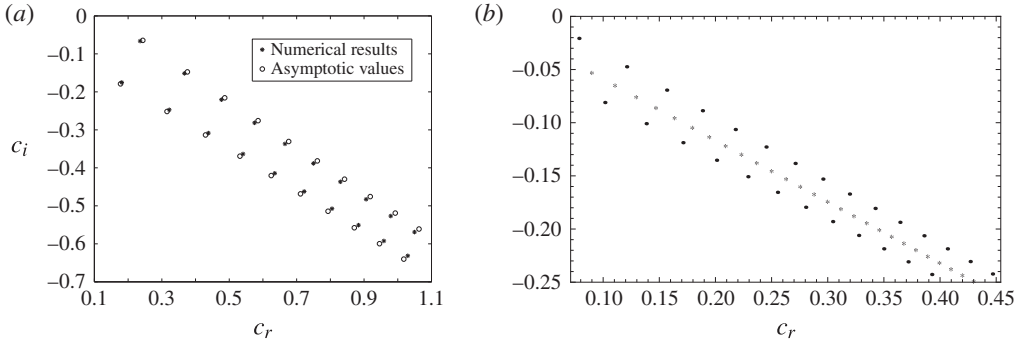

FIGURE 7. The viscous OS spectrum for semi-infinite Couette flow ($U(z) \propto z$ with $0 \leqslant z < \infty$). (*a*) Numerical solutions of (5.14) compared with the asymptotic values given by (5.15) for $Re = 5000$. (*b*) The OS and Squire eigenvalues for $Re = 150\,000$, highlighting the correspondence between the large-Re OS (•) and Squire (∗) spectra.

that remain at an $O(1)$ distance from the real axis. In this sense, there are no qualitative differences in the viscous–inviscid relation for Couette flow in bounded and semi-infinite domains.

5.2. *Viscous spectrum of the Orr–Sommerfeld equation*

For the OS spectrum, we solve (5.8), but with $\Phi \propto \hat{w}_{y'}$. For a semi-infinite domain, $\Phi(z) = \mathrm{Ai}[(\mathrm{i}Re)^{1/3}\{z - c + (\mathrm{i}Re)^{-1}\}]$ as before, with the normal velocity given by

$$\hat{u}_z(z) = -\frac{1}{2k}\left[\mathrm{e}^{-kz}\int_0^z (\mathrm{e}^{kz'} - \mathrm{e}^{-kz'})\mathrm{Ai}[(\mathrm{i}Re)^{1/3}\{z' - c + (\mathrm{i}Re)^{-1}\}]\,\mathrm{d}z' + (\mathrm{e}^{kz} - \mathrm{e}^{-kz})\int_z^\infty \mathrm{e}^{-kz'}\mathrm{Ai}[(\mathrm{i}Re)^{1/3}\{z' - c + (\mathrm{i}Re)^{-1}\}]\,\mathrm{d}z'\right], \tag{5.13}$$

from use of the appropriate Green's function for the semi-infinite domain. Applying the tangential velocity boundary condition at $z = 0$ leads to the following dispersion relation (Baines, Majumdar & Mitsudera 1996):

$$\int_0^\infty \mathrm{Ai}[(\mathrm{i}Re)^{1/3}\{z' - c_n + (\mathrm{i}Re)^{-1}\}]\,\mathrm{e}^{-z'}\,\mathrm{d}z' = 0. \tag{5.14}$$

For $Re \gg 1$ the above equation yields the following asymptotic estimates for the OS eigenvalues (Drazin & Reid 1981):

$$c_n \sim \mathrm{e}^{-\pi\mathrm{i}/6}Re^{-1/3}[\tfrac{3}{8}\pi(8n-1) \pm \tfrac{3}{2}\mathrm{i}\cosh^{-1}\{\pi(\tfrac{3}{8}(8n-1))^{1/2}\}]^{2/3}, \tag{5.15}$$

where $n = 1, 2, \ldots$. The OS eigenvalues, together with their analytical estimates, are plotted in figure 7(*a*), and the spectrum lies along a pair of approximately parallel rays, starting from close to the origin, at an angle of approximately $\pi/6$. Figure 7(*b*) shows the relation between the OS and Squire spectra for $Re = 150\,000$, a value high enough to emphasize the correspondence between the two eigenvalue sequences. For $Re \to \infty$, with $c_i \sim O(1)$, $n \sim O(Re^{1/2})$, it may be shown from (5.15) that the two OS rays are separated by an asymptotically small distance of $O((\log Re)/Re^{1/2})$, and, except for a

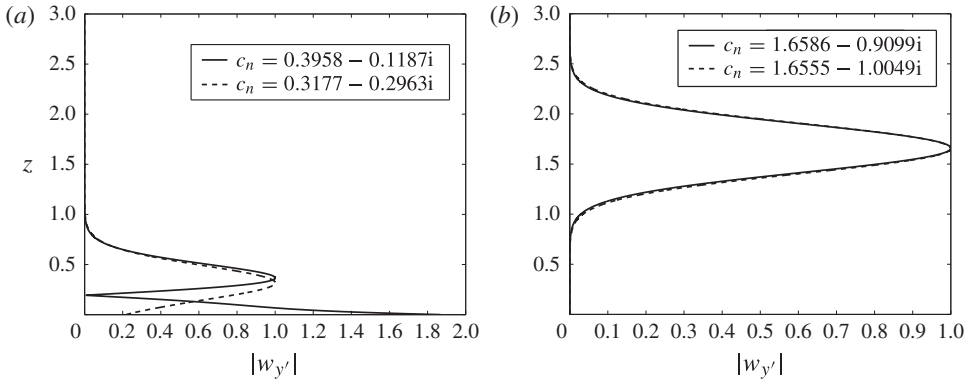

FIGURE 8. Amplitude plots for the wavevector inclined vorticity ($\hat{w}_{y'}$) eigenfunctions for the (a) first and (b) ninth OS mode pairs; $Re = 1000$.

region of $O(Re^{-1/3})$ in the vicinity of the origin, must therefore approach the single ray $\theta = \pi/6$ found for the Squire case. Note that the spacing between successive OS eigenvalues, along the rays, decreases at an asymptotically faster rate as ($O(Re^{-5/6})$) than the inter-ray separation.

The amplitude plots in figure 8(a) emphasize the distinction between a pair of wall modes; the two modes, in fact, exhibit phase contours of opposing inclinations in an $O(Re^{-1/3})$ wall boundary layer (see Baines *et al.* 1996). In contrast, figure 8(b) shows the $\hat{w}_{y'}$ fields for a pair of interior OS modes to be nearly coincident at large Re. The coincidence of the Squire and OS interior eigenmodes is expected for large Re since, in either case, the structure of the vorticity field arises from a local balance of convection and diffusion, with the direct effect of the (differing) boundary conditions being exponentially small. As a result, an expansion similar to (5.11) must continue to hold to within an exponentially small error, with the delta function in (5.11) now corresponding to the $\hat{w}_{y'}$ field. Note that each OS wavepacket has a spatial extent of $O(Re^{-1/3})$, which is asymptotically greater than the $O(Re^{-1/2})$ differences between the OS and Squire eigenvalues. In the limit of large Re, therefore, (5.11) also corresponds to the relation between an inviscid Rayleigh (vorticity) eigenmode and the corresponding superposition of the (interior) OS modes.

5.3. *Viscous spectrum in the spanwise limit*

In the earlier subsections, the Squire and OS spectra, for a general inclined wavevector, are seen to consist of spatially localized inviscidly decaying vorticity eigenfunctions with a vertical extent of $O(Re^{-1/3})$. The $O(Re^{-1/3})$ scale results from a balance between shear, projected along $\boldsymbol{k}$, and viscous diffusion. However, with Re fixed, the spatial extent of the originally localized wavepackets increases without bound for $\psi \to \pm\pi/2$ owing to the vanishing effect of the shear for streamwise-uniform disturbances. Such disturbances require special consideration, and we now examine the viscous–inviscid relation for $\psi = \pi/2$.

In the spanwise limit, a bounded domain is a better starting point. Use of the modal form $\phi(\boldsymbol{x}, t) = \Phi(z)\,\mathrm{e}^{\mathrm{i}(k_y y + \omega t)}$ in (5.3), the inverse spanwise wavenumber (k_y^{-1}) as a characteristic inverse length scale and $(\nu k_y^2)^{-1}$ as a characteristic time scale leads to

the following Squire eigenvalue problem:

$$\frac{\mathrm{d}^2\Phi}{\mathrm{d}z^2} = (1 + \mathrm{i}\omega)\Phi, \tag{5.16}$$

with $\Phi(0) = \Phi(k_yH) = 0$, H being the vertical extent of the domain. The structure of a spanwise Squire eigenmode is evidently independent of Re. It is readily shown that the Squire eigenvalues are given by $\omega_n = \mathrm{i}(1 + n^2\pi^2/(k_yH)^2)$, consistent with diffusive decay. Even and odd n values correspond to the odd and even Squire modes (with regard to their z dependence relative to $z = H/2$), respectively. The OS eigenvalue problem is again characterized by (5.16), but with Φ now denoting the streamwise vorticity component, and with the boundary conditions $\int_0^{k_yH} \sinh z'\,\Phi(z')\,\mathrm{d}z' = \int_0^{k_yH} \sinh(z' - k_yH)\Phi(z')\,\mathrm{d}z' = 0$. The latter correspond to the z derivative of the normal velocity vanishing at each boundary; as in § 5.2, the corresponding conditions for $\hat{u}_z$ are automatically satisfied on use of the bounded-domain Green's function. The resulting dispersion relations are given by

$$p\tan\left(p\frac{k_yH}{2}\right) + \tanh\left(\frac{k_yH}{2}\right) = 0, \tag{5.17}$$

$$p\cot\left(p\frac{k_yH}{2}\right) - \coth\left(\frac{k_yH}{2}\right) = 0, \tag{5.18}$$

for the even and odd OS modes, respectively, with $\omega = \mathrm{i}(1 + p^2)$. (It appears that the results for the Squire and OS eigenvalues given in Schmid & Henningson (2001, p. 66) are in error.) Each of the equations (5.17) and (5.18) yields a countable infinity of eigenvalues that are a function of the parameter k_yH.

The Squire and the OS vorticity eigenfunctions are now sines and cosines, in sharp contrast to the localized wavepackets obtained earlier for an inclined wavevector. The notion of interior modes no longer applies, and the differing boundary conditions in the two cases must therefore affect the eigenvalues. This is evident from the non-integer solutions of (5.17) and (5.18), in contrast to the harmonic nature of the Squire eigenvalues. The higher eigenvalues of (5.17) approach $\pm(2n)\pi/(k_yH)$ and those of (5.18) approach $\pm(2n+1)\pi/(k_yH)$, although the even and odd modes are transposed in relation to the Squire spectrum. In the limit of an unbounded domain ($k_yH \to \infty$), both the Squire and OS spectra approach a continuum parametrized as $\omega = \mathrm{i}(1 + r)$ with $r \in (0, \infty)$, and this remains true both for a semi-infinite domain and in the absence of boundaries.

The relation between the spanwise inviscid and viscous modes may now be seen for both the Squire and OS cases from the respective resolutions of the delta function (the inviscid vorticity mode in both cases). Both operators are self-adjoint, with the OS operator being self-adjoint at the level of the velocity (rather than vorticity) eigenfunctions. For the bounded domain, the Squire relation reduces to the usual sine series representation:

$$\delta(z - z_1) = \frac{2}{k_yH}\sum_{n=1}^{\infty} \sin\left(\frac{n\pi z}{k_yH}\right)\sin\left(\frac{n\pi z'}{k_yH}\right). \tag{5.19}$$

For the OS case, for a bounded domain, one may write an arbitrary function $f(z)$ formally in the following form in terms of the normalized OS velocity eigenfunctions:

$$f(z) = \sum_{p_n} \left(\int_0^{k_y H} f(z') \hat{u}_{zn}^{even}(z')\, \mathrm{d}z' \right) \hat{u}_{zn}^{even}(z) + \sum_{q_n} \left(\int_0^{k_y H} f(z') \hat{u}_{zn}^{odd}(z')\, \mathrm{d}z' \right) \hat{u}_{zn}^{odd}(z). \tag{5.20}$$

Here we have used p_n and q_n to denote the eigenvalues for the even and odd modes, the OS velocity eigenfunctions being given by

$$\begin{aligned} \hat{u}_{zn}^{even}(z) &= N_n^{even} \left[2 \sin\left(p_n \frac{k_y H}{2} \right) \cosh\left(\frac{k_y H}{2} \right) \sinh\left(z - \frac{k_y H}{2} \right) \right. \\ &\quad \left. - \sinh(k_y H) \sin\left\{ p_n \left(z - \frac{k_y H}{2} \right) \right\} \right], \end{aligned} \tag{5.21}$$

$$\begin{aligned} \hat{u}_{zn}^{odd}(z) &= N_n^{odd} \left[2 \cos\left(p_n \frac{k_y H}{2} \right) \sinh\left(\frac{k_y H}{2} \right) \cosh\left(z - \frac{k_y H}{2} \right) \right. \\ &\quad \left. - \sinh(k_y H) \cos\left\{ p_n \left(z - \frac{k_y H}{2} \right) \right\} \right], \end{aligned} \tag{5.22}$$

where N^{even} and N^{odd} are normalization constants with a rather complicated dependence on the eigenvalues and $k_y H$. One may now take $f(z) \propto \mathrm{e}^{-|z-z_1|}$ in (5.20), and operate both sides with $(\mathrm{d}^2/\mathrm{d}z^2 - 1)$ to obtain the delta function as the following superposition of OS vorticity modes for a bounded domain:

$$\begin{aligned} &\delta(z - z_1) \\ &= \sum_{p_n} (p_n^2 + 1) \sinh(k_y H) N_n^{even} \left(\int_0^{k_y H} \mathrm{e}^{-|z'-z_1|} \hat{u}_{zn}^{even}(z')\, \mathrm{d}z' \right) \cos\left\{ p_n \left(z - \frac{k_y H}{2} \right) \right\} \\ &\quad + \sum_{q_n} (q_n^2 + 1) \sinh(k_y H) N_n^{odd} \left(\int_0^{k_y H} \mathrm{e}^{-|z'-z_1|} \hat{u}_{zn}^{odd}(z')\, \mathrm{d}z' \right) \sin\left\{ q_n \left(z - \frac{k_y H}{2} \right) \right\}, \end{aligned} \tag{5.23}$$

where the cosine and sine functions correspond to the even and odd OS vorticity modes. In the limit $k_y H \to \infty$, both (5.19) and (5.23) reduce to the Fourier integral representation expected for a CS with sinusoidal eigenfunctions (Friedman 1990):

$$\delta(z - z_1) = \int_{-\infty}^{\infty} \sin(l\pi z) \sin(l\pi z_1)\, \mathrm{d}l. \tag{5.24}$$

For any finite time, the evolution in terms of the viscous modes is given by

$$\mathcal{G}_{sp}(z, t; z_1) = \mathrm{e}^{-\nu k_y^2 t} \int_{-\infty}^{\infty} \sin(l\pi z) \sin(l\pi z_1)\, \mathrm{e}^{-\nu l^2 \pi^2 t}\, \mathrm{d}l, \tag{5.25}$$

$$= \frac{\mathrm{e}^{-\nu k_y^2 t}}{\sqrt{\pi \nu t}} \left\{ \exp\left[-\frac{(z - z_1)^2}{4\nu t} \right] - \exp\left[-\frac{(z + z_1)^2}{4\nu t} \right] \right\}. \tag{5.26}$$

In (5.24) and (5.26) we revert to dimensional variables to emphasize the dependence of the decay rates on ν alone. The l-independent exponential prefactor ($\mathrm{e}^{-\nu k_y^2 t}$) arises

from the viscous decay due to the spanwise modulation. Equation (5.26) is the analogue of (5.6) in the absence of shear (with the image contribution included to satisfy the boundary conditions), and suggests an alternative interpretation of the dynamics in terms of a diffusively broadening wavepacket, as originally found by Murdock & Stewartson (1977) for Blasius-like flow profiles.

To summarize, (5.11) and (5.12) for perturbations with an inclined wavevector, and (5.24) and (5.25) for streamwise-uniform perturbations, are the main results of this section. They relate the inviscid and viscous modal interpretations, both at the initial instant and at later times, for Couette flow. It is worth commenting briefly if the features of the large-Re spectrum found here (spatially localized eigenfunctions and movement of the eigenvalues towards the boundaries with increasing Re) persist for a general non-inflectional shearing flow; note that the onset of the Tollmien–Schlichting instability is a detail in this context, since this only involves a weakly damped wall mode on the A branch (see below) crossing over to the unstable side. That this might be so stems from two facts: first, the spatial localization of the Couette eigenfunctions arises from a local balance between shear and viscous diffusion, and this is likely to hold even for a nonlinear flow; second, inviscidly decaying quasi-modes are an exceptional occurrence (Stewartson 1981). For a bounded domain, the spectrum for a general shearing flow in a bounded domain exhibits a Y-shaped structure with the two branches (A and P) and a stem (the S branch); Couette flow is a degenerate example, with two A branches instead (Schmid & Henningson 2001). There does exist numerical evidence for the invariance of the Y-shape for plane Poiseuille flow (figure 5 in Reddy *et al.* 1993). For Blasius-like profiles in a semi-infinite domain, there is only an A branch and a vertical line corresponding to the viscous CS with modes that propagate at the free-stream velocity (Mack 1976; Grosch & Salwen 1978). Murdock & Stewartson (1977), via the analysis of a piecewise uniform flow in a semi-infinite domain ($U(z) = \mathcal{H}(1-z)$ for $0 \leqslant z < \infty$, $\mathcal{H}$ being the Heaviside function), showed that discrete eigenvalues spring out of the CS and move towards the wall (along the A branch) with increasing Re.

6. Conclusion

In this paper we have given a modal interpretation of the 'lift-up' effect based on the normal modes of the Rayleigh and inviscid Squire operators. This involved identifying the two inviscid (Rayleigh and Squire) CS for a non-inflectional shearing flow in § 3 – the wavevector-aligned version of the so-called Case vortex sheets (see § 3.1) and the Squire jets (needed for perturbations with a spanwise component of variation; see § 3.2). An arbitrary initial condition was expanded in terms of these two eigenmode families (see § 4.1). The limiting form of this expansion was used to show how a streamwise-uniform 'roll' initial condition leads to an inviscid algebraic instability (see § 4.2). The formulation was then expanded to include discrete modes for inflectional profiles (§ 4.3). In § 5, a detailed connection was made between an inviscid CS mode and a collection of viscous discrete modes, for Couette flow in a semi-infinite domain. This viscous–inviscid relation reduces to a simpler form for streamwise-uniform disturbances known from earlier analyses of Blasius-like profiles (Murdock & Stewartson 1977).

A point that needs emphasis is the non-convergence of the viscous (OS and Squire) spectra to the corresponding inviscid ones (Rayleigh and inviscid Squire) even in the limit of infinite Re. As a result, a connection can only be established between an inviscid eigenmode and an (infinite) superposition of viscous discrete modes.

The viscous–inviscid relation was examined in § 5 to show how the interpretation of the lift-up effect in terms of non-orthogonal viscous discrete modes (Schmid & Henningson 2001) relates to the explanation presented here in terms of the inviscid CS. Although the two modal interpretations yield the same result, the inviscid one is superior at large Re, since the underlying modes are independent of Re, and the structure of the vorticity field is not crucially dependent on the boundaries. This is in sharp contrast to the viscous case, where the individual modes are not well defined in the limit $Re \to \infty$ except in the streamwise-uniform limit. The nature of the spectrum is itself sensitively dependent on the presence of boundaries, and on the inclination of the wavevector relative to the flow direction. The 'inefficiency' of the viscous modal superposition in representing transient growth dynamics at large Re may also be inferred from the phase plots (not included here). As already seen, transient growth results from either the degree of coherence increasing with time starting from an initial condition with an upstream tilt (Orr), or from vertically coherent roll initial conditions with only a spanwise variation (lift-up). In contrast, for a general inclined wavevector, the phase contours of the viscous discrete modes reveal a pronounced downstream tilt at large Re, leading to an asymptotically small vertical scale of $O(Re^{-1/3})$. Considering a plane wave (Kelvin mode) as given in (5.7), the turning wavevector leads to $k_z \sim O(k_x t)$. With $k_y \sim O(1)$, a vertical length scale of $k_z^{-1} \sim O(Re^{-1/3})$ results only after an asymptotically long time of $O(Re^{1/3})$ when the onset of viscous effects in wall boundary layers prevents further fine scaling, leading to a permanent propagating structure characteristic of a normal mode. This is, however, also the time at which transient growth ceases and there is the onset of viscous decay. In this sense, transient growth dynamics and the viscous discrete modes correspond naturally to mutually exclusive intervals of time, and attempting a viscous modal superposition at large Re, to describe transient growth, amounts to representing a vertically coherent or an upstream-tilted perturbation with a set of eigenfunctions each of which has a pronounced downstream tilt. Such a limitation is evidently absent in the inviscid interpretation.

REFERENCES

ABRAMOWITZ, M. & STEGUN, I. A. 1965 *Handbook of Mathematical Functions with Formulas, Graphs and Mathematical Tables*. Dover.

ANDERSSON, P., BERGGREN, M. & HENNINGSON, D. S. 1999 Optimal disturbances and bypass transition in boundary layers. *Phys. Fluids* **11**, 134–150.

ANTKOWIAK, A. & BRANCHER, P. 2004 Transient growth for the Lamb–Oseen vortex. *Phys. Fluids* **16**, L1–L4.

ARNOL'D, V. I. 1972 Notes on the three-dimensional flow pattern of a perfect fluid in the presence of a small perturbation of the initial velocity field. *Z. Angew. Math. Mech.* **36**, 236–242.

BAINES, P. G., MAJUMDAR, S. J. & MITSUDERA, H. 1996 The mechanics of the Tollmien–Schlichting wave. *J. Fluid Mech.* **312**, 107–124.

BALMFORTH, N. J. & MORRISON, P. J. 1995 Singular eigenfunctions for shearing fluids I. *Report* No. 692, Institute for Fusion Studies, University of Texas, Austin.

BENNEY, D. J. & LIN, C. C. 1960 On the secondary motion induced by oscillations in a shear flow. *Phys. Fluids* **3**, 656–657.

CASE, K. M. 1959 Plasma oscillations. *Ann. Phys. (NY)* **7**, 349–364.

CASE, K. M. 1960 Stability of inviscid plane Couette flow. *Phys. Fluids* **3**, 143–148.

DICKINSON, R. E. 1970 Development of a Rossby wave critical level. *J. Atmos. Sci.* **27**, 627–633.

DRAZIN, P. G. & REID, W. H. 1981 *Hydrodynamic Stability*. Cambridge University Press.

ELLINGSEN, T. & PALM, E. 1975 Stability of linear flow. *Phys. Fluids* **18**, 487–488.

FADEEV, L. D. 1971 On the theory of the stability of stationary plane-parallel flows of an ideal fluid. *Zap. Nauch. Semin. Leningrad. Otdel. Mat. Inst. Akad. Nauk SSSR* **21**, 164–172.

FARRELL, B. F. 1987 Developing disturbances in shear. *J. Atmos. Sci.* **45**, 2191–2199.

FARRELL, B. F. & IOANNOU, P. J. 1993 Optimal excitation of three-dimensional perturbations in viscous constant shear flow. *Phys. Fluids* A **5**, 1390–1400.

FRIEDMAN, B. 1990 *Principles and Techniques of Applied Mathematics*. Dover.

GAKHOV, F. D. 1990 *Boundary Value Problems*. Dover.

GROSCH, C. E. & SALWEN, H. 1978 The continuous spectrum of the Orr–Sommerfeld equation. Part 1. The spectrum and the eigenfunctions. *J. Fluid Mech.* **87**, 33–54.

GROSCH, C. E. & SALWEN, H. 1981 The continuous spectrum of the Orr–Sommerfeld equation. Part 2. Eigenfunction expansions. *J. Fluid Mech.* **104**, 445–465.

JIMENEZ, J. & PINELLI, A. 1999 The autonomous cycle of near wall turbulence. *J. Fluid Mech.* **389**, 335–359.

KELBERT, M. & SAZONOV, I. 1996 *Pulses and Other Wave Processes in Fluids*. Kluwer.

LANDAHL, M. T. 1980 A note on an algebraic instability of inviscid parallel shear flows. *J. Fluid Mech.* **98**, 243–251.

LEE, M. J., KIM, J. & MOIN, P. 1990 Structure of turbulence at high shear rate. *J. Fluid Mech.* **216**, 561–583.

LIGHTHILL, M. J. 1958 *An Introduction to Fourier Analysis and Generalized Functions*. Cambridge University Press.

LIN, C. C. 1955 *The Theory of Hydrodynamic Stability*. Cambridge University Press.

LINDZEN, R. S. 1988 Instability of plane parallel shear flow (toward a mechanistic picture of how it works). *Pure Appl. Geophys.* **126**, 103–121.

MACK, L. M. 1976 A numerical study of the temporal eigenvalue spectrum of the Blasius boundary layer. *J. Fluid Mech.* **73**, 497–520.

MARCUS, P. S. & PRESS, W. H. 1977 On Green's functions for small disturbances of plane Couette flow. *J. Fluid Mech.* **79**, 525–534.

MOFFATT, H. K. 1965 The interaction of turbulence with rapid uniform shear. *Report* No. SUDAER-242, Department of Aeronautics and Astronautics, Stanford University, CA.

MURDOCK, J. W. & STEWARTSON, K. 1977 Spectra of the Orr–Sommerfeld equation. *Phys. Fluids* **20**, 1404–1411.

PRADEEP, D. S. & HUSSAIN, F. 2006 Transient growth of perturbations in a vortex column. *J. Fluid Mech.* **550**, 251–288.

REDDY, S. C., SCHMID, P. J. & HENNINGSON, D. S. 1993 Pseudospectra of the Orr–Sommerfeld operator. *SIAM J. Appl. Maths* **53**, 15–47.

RESHOTKO, E. 2001 Transient growth: a factor in bypass transition. *Phys. Fluids* **13**, 1067–1075.

ROGERS, M. M. & MOIN, P. 1987 The structure of the vorticity field in homogeneous turbulent flows. *J. Fluid Mech.* **176**, 33–66.

ROY, A. 2013 Singular eigenfunctions in hydrodynamic stability: the roles of rotation, stratification and elasticity. PhD thesis, Jawaharlal Nehru Centre for Advanced Scientific Research.

ROY, A. & SUBRAMANIAN, G. 2014 Linearized oscillations of a vortex column: the singular eigenfunctions. *J. Fluid Mech.* **741**, 404–460.

SAZONOV, I. A. 1989 Interaction of continuous spectrum waves with each other and discrete spectrum waves. *Fluid Dyn. Res.* **4**, 586–592.

SAZONOV, I. A. 1996 Evolution of three-dimensional wavepackets in the Couette flow. *Izv. Acad. Nauk SSSR Atmos. Ocean. Phys.* **32**, 21–28.

SCHMID, P. J. & HENNINGSON, D. S. 2001 *Stability and Transition in Fluid Flows*. Springer.

STAKGOLD, I. 1968 *Boundary Value Problems of Mathematical Physics*. Macmillan.

STEWARTSON, K. 1981 Marginally stable inviscid flows with critical layers. *IMA J. Appl. Maths* **27**, 133–175.

TUMIN, A. & RESHOTKO, E. 2001 Spatial theory of optimal disturbances in boundary layers. *Phys. Fluids* **13**, 2097–2104.

TUNG, K. K. 1983 Initial-value problems for Rossby waves in a shear flow with critical level. *J. Fluid Mech.* **133**, 443–469.